Journal of Translational Medicine

RESEARCH

Open Access

FOSL1 drives the malignant progression of pancreatic cancer cells by regulating cell stemness, metastasis and multidrug efflux system

Xiaolong Liu[1†], Xueyan Zhang[2†], Tingyu Zeng[2], Yali Chen[2], Liu Ye[3], Shuping Wang[2*] and Yulan Li[1*]

Abstract

Background Targeted therapy is an effective strategy for the treatment of advanced and metastatic pancreatic cancer, one of the leading causes for cancer-related death worldwide. To address the limitations of existing targeted drugs, there is an urgently need to find novel targets and therapeutic strategies. Transcription factor FOS like 1 (FOSL1) is a potential therapeutic target for challenging pancreatic cancer, which contributes to the malignant progression and poor gnosis of pancreatic cancer. High mobility group A1 (HMGA1) is a nonhistone chromatin structural protein that contributes to malignant progression and poor prognosis of cancer.

Methods Human FOSL1 complete RNA, shRNA against FOSL1 and shRNA against HMGA1 lentiviral recombination vectors were used to overexpress FOSL1 and knock down FOSL1 and HMGA1. RNA sequencing, Q-PCR and Western blots were used to investigate the mechanism of FOSL1 in regulating the proliferation of pancreatic cancer cells. The relationship between FOSL1 and HMGA1 were analyzed by co-immunoprecipitation Mass spectrometry, Q-PCR of chromatin immunoprecipitation and Western blots. The regulation of FOSL1 and HMGA1 in the invasion and migration, stemness, and multidrug efflux system were determined by transwell assay, sphere formation assay, immunofluorescence, Q-PCR and Western blots.

Results We found that FOSL1 promoted the proliferation and progression of pancreatic cancer by trigging stemness, invasion and metastasis, and drug resistance. HMGA1 was a key downstream target regulated by FOSL1 at the transcriptional level and directly interacted with FOSL1. Knockdown of HMGA1 inhibited the proliferation of pancreatic cancer cells by regulating the expression of genes related to stemness, epithelial-mesenchymal transition and multidrug efflux system. Targeted inhibition of FOSL1 and HMGA1 expression significantly inhibited the proliferation of pancreatic cancer cells.

†Xiaolong Liu and Xueyan Zhang contributed equally to this work.

*Correspondence:
Shuping Wang
wangsp@lzu.edu.cn
Yulan Li
liyul@lzu.edu.cn

Full list of author information is available at the end of the article

Conclusion FOSL1 promote the malignant progression of pancreatic cancer by promoting HMGA1 expression. Targeting FOSL1 and HMGA1 in monotherapy or combination therapy is a promising strategy for the treatment of advanced and metastasis pancreatic cancer.

Keywords Pancreatic cancer, FOSL1, HMGA1, Stemness, Drug resistance, Metastasis

Introduction

Pancreatic cancer is one of the leading causes for cancer-related death worldwide [1]. With the rising incidence, pancreatic cancer is predicted to become the second leading cause of cancer death in the next decade [1–2]. Due to the lack of specific symptoms and effective diagnostic methods in the early stage, pancreatic cancer is usually detected in advanced stage and has poor five-year survival and prognosis [1–3]. The poor prognosis of pancreatic cancer is due to its early systemic spread and aggressive local growth [1–3]. Majority of pancreatic cancer patients have unresectable or metastatic lesions, and only 10–15% of pancreatic cancer patients have localized lesions [1–4]. Currently, surgery is still the main treatment for pancreatic cancer patients with local lesions. With the updating of minimally invasive techniques and surgical adjuncts, the quality and safety of pancreatic cancer surgery have been improved in recent years [1–3]. Gemcitabine, 5-fluorouracil and oxaliplatin are mainly used in the first-line treatment of advanced and metastatic pancreatic cancer and as adjuvant therapy after complete resection of the primary tumor [4, 5]. Although the initial efficacy of systemic chemotherapy is well, most pancreatic cancer patients develop resistance to these chemotherapeutic agents, further increasing the difficulty of treatment and poor prognosis. At the same time, the side effects of systemic chemotherapy seriously affect the life quality of patients [4, 5]. With the development of sequencing technology and bioinformatics, the driving mutations and abnormal pathways of pancreatic cancer are rapidly discovered [6–9]. Innovative targeted therapies have the potential to improve survival and quality of life for patients with pancreatic cancer. Pancreatic cancer patients with mutations in DNA damage repair pathways have been showed not only to be sensitive to platinum-based therapy, but also to benefit from PARP inhibitors, such as Olaparib [4–7]. Targeting KRAS mutations is proving to be another effective strategy for treating pancreatic cancer, which is present in about 95% of patients [6–9]. Clinically, Sotorasib has been shown to be effective in pancreatic ductal adenocarcinoma (PDAC) patients with KRAS G12C mutations [9]. The success of PARP targeted therapy and KRAS targeted therapy demonstrates the importance of targeted therapy in the treatment of advanced pancreatic cancer. However, existing targeted drugs have limitations such as narrow clinical indications and drug resistance [6–9]. Therefore, novel targets and therapeutic strategies are urgently required for the treatment of challenging pancreatic cancer.

FOS-like antigen 1 (FOSL1) belongs to the activator protein 1 (AP1) transcription factor family [10]. AP1 is a dimeric transcription factor composed of Jun proto-oncogene (JUN) family, FOS family and activating transcription factor protein families [10–12]. It is well known that AP1 family proteins can promote oncogenesis in a variety of cancers, especially FOSL1 and JUN, which are highly expressed in metastatic cancers and can mediate the proliferation and metastasis of cancers [10–12]. FOSL1 has been reported to control various pathophysiological processes by regulating downstream gene expression [10–12]. FOSL1 is overexpressed in many human cancers and contributes to malignant progression and poor prognosis by modulating cancer cell metastasis, stemness and chemotherapy resistance [13–17]. For example, overexpression of FOSL1 promotes the malignant progression and poor prognosis of mutant KRAS lung and pancreatic cancer [18]. FOSL1 has been shown to cause the metastasis of head and neck squamous cell carcinoma, enhance the stemness of glioma, promote 5-Fu resistance in colon cancer cells, and result in drug resistance of breast cancer [14–17]. Notably, FOSL1 has been shown to promote the malignant proliferation and metastasis of pancreatic cancer, but the mechanism is unclear [19, 20]. Based on the above results, this study will further explore the role and mechanism of FOSL1 in the malignant progression of pancreatic cancer.

High mobility group A1 (HMGA1) is a nonhistone chromatin structural protein that performs regulatory roles by modifying DNA structure [21]. HMGA1 is overexpressed in proliferative cells such as embryos and cancers [21, 22]. Indeed, HMGA1 has been shown to promote carcinogenesis in reproductive system, digestive system, urinary system and hematopoietic system by regulating the expression of tumor-related genes [21–23]. HMGA1 results in malignant progression and poor prognosis of cancers by promoting cancer cell stemness, metastasis, drug resistance, immunosuppression, and cell cycle progression [22–26]. As for the mechanism, HMGA1 exerts its cancer-promoting function through Wnt/β-catenin, phosphatidyl inositol 3-kinase (PI3K)/protein kinase B (AKT), and mitogen-activated protein kinase kinase (MEK)/ extracellular regulated protein kinases (ERK) pathways [27–29]. So far, many studies have shown that HMGA1 is overexpressed in pancreatic cancer and is closely related to the progression and

metastasis of pancreatic cancer [30]. This suggests that HMGA1 is another essential target for pancreatic cancer progression and poor prognosis. Based on previous studies, we will investigate the mechanism of HMGA1 regulating the proliferation of pancreatic cancer.

In this study, we investigated the role of FOSL1 in regulating the malignant progression and poor prognosis of pancreatic cancer. FOSL1 facilitated the progression of pancreatic cancer by promoting the stemness, invasion and migration of cancer cells, and regulating the multidrug efflux system. The results of RNA sequencing and Co-immunoprecipitation (Co-IP) Mass spectrometry showed that HMGA1 was a key target that regulated by FOSL1 and directly interacted with FOSL1. Q-PCR of chromatin immunoprecipitation (ChIP) confirmed that the promoter of HMGA1 directly binds to FOSL1. HMGA1 is directly regulated by FOSL1 at the transcriptional level. Further experiments confirmed that FOSL1 promoted the proliferation of pancreatic cancer cells by promoting HMGA1 expression. Knockdown of HMGA1 inhibited the proliferation, stemness, invasion and migration of pancreatic cancer cells, blocked the expression of genes related to multidrug efflux system, and promoted the apoptosis of pancreatic cancer cells. Moreover, targeted inhibition of FOSL1 and HMGA1 expression significantly inhibited the proliferation of pancreatic cancer cells. Our study provides innovation insights into targeted therapies for pancreatic cancer. Targeting FOSL1 and HMGA1 in monotherapy or combination therapy should be an efficient strategy for the treatment of advanced and metastasis pancreatic cancer.

Materials and methods

Cell culture

The human pancreatic cancer cells lines SW1990 and PANC-1 cells were purchased from the cell resources center of shanghai academy of life sciences (Shanghai, China). Capan-1 cells and HPNE cells were purchased from Langfang Beina Biotechnology Co., Ltd (Hebei, China). PANC-1 cells were cultured in DMEM (KGL1206, KeyGEN Biotech, Nanjing, Jiangsu, China) with 10% fetal bovine serum (FBS). SW1990 cells were cultured in Leibovitz's L-15 (KGL1804, KeyGEN Biotech, Nanjing, Jiangsu, China) with 10% FBS. Capan-1 cells were cultured in IMDM (KGL1101, KeyGEN Biotech, Nanjing, Jiangsu, China) with 15% FBS. HPNE cells were cultured in RPMI-1640 (KGL1501, KeyGEN Biotech, Nanjing, Jiangsu, China) with 10% FBS. All cells were incubated at 37 °C in a 5% CO_2 atmosphere.

Bioinformatics data mining and analysis

The differential expression of genes in the cancer genome atlas (TCGA) database was analyzed by Gene Expression Profiling Interactive Analysis (GEPIA) online website (http://gepia2.cancer-pku.cn/#index). The mRNA expression of FOSL1 and other genes in clinical cancer samples was compared with that in normal adjacent from TCGA database, and the P value was obtained by one-way ANOVA. The significant values of *P*-value and folding change are 0.05 and 2.0 respectively. The effects of FOSL1 and other genes on the survival of patient with pancreatic cancer were valuated using Kaplan-Meier Plotter. Samples were divided into two groups with high expression and low expression according to the median expression. The 95% confidence interval (CI), log rank risk ratio (HR) and P value of overall survival and disease-free survival were evaluated. The relationship between gene expression and prognosis was analyzed by the receiver operating characteristic (ROS) curves. The original clinical data source of 183 pancreatic cancer RNA sequencing information was obtained from the TCGA database (https://portal.gdc.com). The ROS curves and calculated area under the curve (AUC) values were analyzed by the R package pROC, and the data were visualized as ggplot2. The AUC value between 0.5 and 0.7 indicates evidence of model success, the value between 0.7 and 0.9 indicates strong evidence of model success, and the value greater than 0.9 indicates strong evidence of model success [31]. Statistical analysis and visualization were performed in R version 3.6.3. The expression correlation between the key genes of interest in the previous intersection genes and FOSL1 expression were analyzed by the GEPIA2 online tool. The expression distribution of FOSL1 mRNA in different pancreatic cancer cell lines was obtained from the CCLE dataset (https://portals.broadinstitute.org/ccle). The analysis was constructed by the R v4.0.3 software ggplot2 (V3.3.3). The ChIP-seq data for FOSL1 was obtained from the Cistrome Data Browser (http://cistrome.org/db/#/).

RNA sequencing and data processing of DEGs

PANC-1 cells were transfected with short-hairpin RNA against FOSL1 (FOSL1 shRNA) or NC shRNA for 3 days. After treatment, cells were collected to obtain total RNA using TRIzol reagent (Vazyme, Nanjing, China) according to the manufacturer's manual. A total of 600 ng RNA was used to prepare libraries using the NEBNext Ultra RNA Library Perp Kit for Illumina. RNA quantity and quality were assessed on an Agilent 2100 Bioanalyzer. RNA library sequencing was performed on an Illumina HiSeqTM 2500/4000 by Gene Denovo Biotechnology Co., Ltd. (Guangzhou, Guangdong, China). Differentially expressed genes (DEGs) in the NC shRNA group vs. the FOSL1 shRNA group were identified based on a$|\log_2FC|>1.0$ and an adjusted $P<0.05$. DEGs with a $\log_2FC<1.0$ were considered downregulated genes, while DEGs with a $\log_2FC>1.0$ were considered upregulated genes [32, 33]. The raw sequencing data of RNA-seq has been uploaded onto SRA database (accession number: PRJNA1217410).

GO, KEGG pathway and GESA enrichment analysis

The characteristic biological attributes of the DEGs were identified by gene ontology (GO) enrichment and gene set enrichment analysis (GESA) enrichment analysis. The functional attributes of the DEGs were identified by kyoto encyclopedia of genes and genomes (KEGG) pathway enrichment and GESA enrichment analysis. GO enrichment analysis, KEGG pathway enrichment analysis and GESA enrichment analysis were performed using Omicsmart, a real-time interactive online platform for data analysis (http://www.omicsmart.com) [31, 32].

Lentivirus transfection

Lentiviral recombination vectors of human FOSL1 complete RNA (FOSL1 cRNA) (pGV492-FOSL1), HMGA1 cRNA (pGV492-HMGA1) and its scrambled control (pGV492-NC), Lentiviral recombination vectors of shRNA against FOSL1 (pGV248-shFOSL1), shRNA against HMGA1 (pGV248-shHMGA1) and the scrambled control (pGV112-shNC) were constructed and purchased from Genechem Co. Ltd. (Shanghai, China). The Lentiviral vector of GV492-FOSL1 and GV492-HMGA1 was confirmed by PCR and sequencing. The pGV248-shFOSL1 vector and pGV248-shHMGA1 vector were confirmed by sequencing. PANC-1 cells and SW1990 cells were infected with FOSL1 cRNA, HMGA1 cRNA, NC cRNA, FOSL1 shRNA, HMGA1 shRNA and NC shRNA Lentiviral vectors using HitransG P promoting reagent according to the manufacturer's instructions. After infection with lentiviral vector for 3 days, culture medium containing virus was removed. Transfected cells were allowed for growth for 3–5 days, and then treated with 2.0 μg/mL puromycin for 24 h to select positive infected cells. For the rescue experiment, cells were infected with one lentiviral vector for 3 days and the culture medium containing virus was removed. The cells were then infected with another vector for 3 days, and the culture medium containing virus was removed. Cells transfected with two vectors were allowed for growth for 3–5 days, and then applied for experiments. All transfected cells were validated by Q-PCR and Western blots, and maintained in medium containing 1.0 μg/mL puromycin [30, 31]. The target sequence of FOSL1 shRNA is 5'-CTGTACCTTGTATCTCCCTTT-3', target sequence of HMGA1 shRNA is 5'- CAACTCCAGGAAGGAAAC CAA-3', target sequence of NC shRNA is5'- CA TTCTC CGAACGTGTCACGT – 3'.

MTT assay for cell viability

Cell viability in each group was analyzed by MTT assay [32, 33]. Untreated cells served as the control. After the cells transfected with lentiviral vector were cultured at different time, the viabilities of PANC-1 cells and SW1990 cells were measured by MTT assay. The relative ratio of MTT assay was calculated by the equation: relative ratio = $A_{Group,\ day}/A_{Control,\ 1}$. Herein, $A_{Group,\ day}$ represents the absorbance value of the comparison group after culture for different days, $A_{Control,\ 1}$ represents the absorbance value of untreated cells after culture for 1 day.

Colony formation assay

All cells were seeded in 6-well plates at a concentration of 500 cells/well. After SW1990 cells and PANC-1 cells were transfected with different lentiviral vectors, the cells were cultured in medium containing 1.0 μM puromycin for 14 days. The culture medium was changed every 3 days to allow colony formation. After treatment for 14 days, the colonies were fixed with cold methanol for 10 min, stained with 0.1% crystal violet for 10 min, and imaged using Live cell imaging system of Bio-Tek (Cytation 5, Vermont, USA). Experiments were repeated at least three times [32, 33].

Cell apoptosis assays

Cell apoptosis was analyzed by Annexin V-FITC and PI apoptosis detection kits (KeyGEN Biotech, Nanjing, Jiangsu, China). After SW1990 cells and PANC-1 cells were transfected with different lentiviral vectors, the cells were cultured in medium containing 1.0 μM puromycin for 3 days. After treatment, the cells were collected and stained with Annexin V-FITC and PI following the manufacturer's protocol to analyze cell apoptosis [32, 33]. Cell apoptosis was detected by Agilent NovoCyte Quanteon (California, USA) flow cytometer or BD LSRFortessa TM (New Jersey, USA) flow cytometer. The data of apoptosis were analyzed by FlowJo 7.6.

Migration and invasion assay

Transwell plate was used to perform cell migration and invasion experiments. After SW1990 cells and PANC-1 cells were transfected with different lentiviral vectors, the cells were cultured in medium containing 1.0 μM puromycin for 3 days. After treatment, the cells were collected and counted to determine cell migration and invasion. For migration, cells (1×10^5/ml) were collected, suspended in 200 μl medium without FBS and seeded into the upper well of the chamber, and the lower well contained culture medium with 10% FBS. For invasion, the upper well of each group was plated with 20 μl Matrigel. After Matrigel solidifying, cells in 200 μl medium without FBS were seeded into the upper well, and the lower well contained culture medium with 10% FBS. After incubation for 48 h, the cells were fixed with 4% formaldehyde for 30 min, stained with Giemsa for 15 min. Cell migration or invasion was observed on the outside of the upper well were observed with a Nikon inverted fluorescence microscope (Ts2R-FL, Tokyo, Japan) following the

manufacturer's introduction. Five images were randomly captured per slide.

Sphere formation assay

After SW1990 cells and PANC-1 cells were transfected with different lentiviral vectors, the cells were cultured in ultra-low attachment plates at a density of 10,000 cells/mL. Cells in each group were maintained in serum-free DMEM/F12 medium supplemented with B27, 20 ng/mL epidermal growth factor (EGF), and 10 ng/mL basic fibroblast growth factor (bFGF) for 14 days. The culture medium was replenished every 4 days by replacing half of the volume to maintain optimal growth conditions. After treatment for 14 days, spheres were imaged using Live cell imaging system of Bio-Tek (Cytation 5, Vermont, USA). Experiments were repeated at least three times [34].

Immunofluorescence (IF) assay

After SW1990 cells and PANC-1 cells were transfected with different lentiviral vectors, the cells were cultured in medium containing 1.0 μM puromycin for 3 days. After treatment, cells were fixed with 4% formaldehyde, permeabilized with 0.2% (v/v) Triton X-100 in PBS, blocked with 1% (w/v) BSA in PBS for 1.0 h and stained with anti-CD44 antibody or anti-ABCB1 antibody overnight at 4 °C, and then stained with Goat Anti-Rabbit IgG H&L labeled with Alexa Fluor 647. After staining, cellular DNA was counterstained with 4,6-diamidino-2-phenylindole (DAPI). Fluorescence signals were detected using a Carl Zeiss LSM900 laser confocal microscope (Jena, Germany). Five fields per sample were quantified.

Table 1 Primer sequences for genes in Q-PCR

Name	Sense (5′-3′)	Antisense (5′-3′)
FOSL1	ACCCATCTGCAAAATCCCGGAA	TGCAGTGCCTCAGGTTCAAGC
CD44	CACAAATGGCTGGTACGTCT	ATCATCAATGCCTGATCCAGA
CD133	TAGCTACATTATCGACCCCTT	AGTACTTAGCCAGTTTTACCG
SOX2	ATGGCCCAGGAGAACCCCAA	TCGCAGCCGCTTAGCCTCGTC
BMI1	TCTTCTTGTTTGCCTAGCC	ATTTACTGATGATTTTCGAGGT
HMGA1	CCAAGCAGGAAAAGGACGGCACT	GGGCTCCTTCTGACTCCCTACCA
CDH1	TGCCGCCATCGCTTACACC	AGGTCAGCAGCTTGAACCAC
CDH2	GAGTTTACTGCCATGACGTT	CTGATTCTGTACACTGCGTTC
CTNNB1	CCACTAATGTCCAGCGTTT	TGGTCCTCGTCATTTAGCAG
VIM	AAATGGCTCGTCACCTTCGT	AAATCCTGCTCTCCTCGCCTT
MMP1	CGCACAAATCCCTTCTACCC	ATCTCTGTCGGCAAATTCGT
ABCB1	AGAACTCTTAGCGTATGCAA	AGAAATATTGGCTGTAATAGCTT
ABCC1	CCTCTATCTCTCCCGACATGACC	GCCCAGCAGACGATCCACA
ABCC4	TTGCACACAGATTGAACACC	ACCATCTTGTAAAATAGGCTCT
ABCG1	GTCGCTCCATCATTTGCACCA	GGCAGTTCAGACCCAAATCCC
ABCG2	TAGCTGCAAGGAAAGATCCAA	ATCTTGTACCACGTAACCTG
SNAL	TCACCGGCTCCTTCGTCCT	CCTTTCGAGCCTGGAGATCCTT
OCT4	CAGATCAGCCACATCGCCCAG	AGCAGCCTCAAAATCCTCTCGTT
ALDH1	CAGTGTTGTATAGCCGCATC	ATATACTTCTTAGCCCGCTCA
FN1	TTTCCCATTATGCCGTTGGAG	AATGACCACTTCCAAAGCCTA
ABCC2	AAACTCGGAATGTGAATAGCC	ACAGAATTCATCACAAACGCAAG
ABCC5	CTTGGGCATTGAATTACCGAAC	AACATTCTCTGCCCATCGTTG
GAPDH	GAAACTGTGGCGTGATGGC	CACCACTGACACGTTGGCAG

Q-PCR analysis

After SW1990 cells and PANC-1 cells were transfected with different lentiviral vectors, the cells were cultured in medium containing 1.0 μM puromycin for 3 days. After treatment, total RNA in each group was extracted with TRIzol reagent (Vazyme, Nanjing, Jiangsu, China) according to the manufacturer's instructions. cDNA was synthesized using HiScript II one step RT-PCR kit (R223-01, Vazyme, Nanjing, China) with 1.0 μg of total RNA in a 20 μl reaction system. The resulting cDNA was diluted 1:4 in nuclease-free water and 2.0 μl was used per Q-PCR reaction with triplicates. Q-PCR was carried out using ChamQ SYBR Q-PCR master mix (Q711-02, Vazyme, Nanjing, China) on a QuantStudio 3 real time PCR detection system (Life Tech, New York, USA) including a nontemplate negative control. GAPDH was used to normalize the level of mRNA expression. The sequences of the primers were listed in Table 1.

Chromatin immunoprecipitation (ChIP) assay

ChIP assay was performed using the Simple ChIP® Plus Sonication Chromatin IP Kit (56383, CST, USA) according to the manufacturer's instructions. In brief, PANC-1 cells were crosslinked with 1% formaldehyde for 15 min. After quenching with glycine solution, the cells were washed and lysed in ChIP Sonication Cell Lysis Buffer. Then, the nucleic fraction was separated from the cell lysate and sheared sonication to fragment the DNA. Chromatin was precipitated by incubating it with anti-FOSL1 antibody or anti-IgG antibody overnight at 4 °C.

The Protein–DNA complexes were enriched and purified by ChIP-Grade Protein G beads. The purified Protein-DNA complexes were de-crosslinked using 5 M NaCl and Proteinase K for 2.0 h at 65 °C. Finally, DNA was purified using spin columns, dissolved in nuclease-free water, and then analyzed by Q-PCR. The primer sequence for HMGA1 was TCAGCCCTGACTCATC CCTC (foreword); CAGTTGTTGGTGTGAGCTCT (reverse).

Western blots analysis

After treatment, total proteins in SW1990 cells and PANC-1 cells were extracted with RIPA cell lysis buffer (Beyotime, Shanghai, China) with added protease/

phosphatase inhibitor cocktail. Protein concentration was determined by the BCA assay, and equal amounts of proteins were loaded for Western blots analysis. In brief, equal amounts of total proteins were loaded for SDS-PAGE and transferred onto a PVDF membrane (Millipore, Billerica, MA, USA). Membranes with protein were blocked with 5% (w/v) skim milk, incubated with primary antibody in Supplementary Materials, and then incubated with secondary antibodies (1:2000) for detection [32, 33]. GAPDH was used to normalize the level of protein expression. Densitometric analysis was performed with ImageJ software.

Co-IP assay

Total proteins were extracted from PANC-1 cells using the lysis/washing buffer in the Protein A/G Magnetic IP/Co-IP kit (ACE Biotechnology, Nanjing, China). Protein A/G magnetic beads were incubated with anti-FOSL1 antibody, anti-HMGA1 antibody and anti-IgG antibody at 4 °C overnight to obtain the anti-FOSL1-Protein A/G magnetic beads, anti-HMGA1-Protein A/G magnetic beads and the anti-IgG-Protein A/G magnetic beads, respectively. Proteins were quantified and adjusted to same concentration, then incubated with the anti-FOSL1-Protein A/G magnetic beads, the anti-HMGA1-Protein A/G magnetic beads, or the anti-IgG-Protein A/G magnetic beads at room temperature for 2 h. After incubation, unbound proteins were washed with IP buffer. For co-IP Mass spectrometry, the resultant protein complexes were separated by SDS-PAGE gel electrophoresis. The in-gel total proteins were analyzed by Gene Denovo Biotechnology Co., Ltd. (Guangzhou, Guangdong, China). For co-IP assay, the resultant protein complexes were subjected to Western blots to determine the interaction between FOSL1 and HMGA1 [32, 33].

In vivo antitumor activity

All animal experiments were carried out in accordance with the institutional guidelines for the care and use of laboratory animals and approved by the committee on the ethics of Animal Experiments of Lanzhou University. Six- to seven-week-old athymic BALB/c-nude mice (16–18 g) were provide by the Animal House in Model Animal Institute of Nanjing University (Nanjing, Jiangsu, China). Mice were bred in an environment with a temperature of 25 °C, relative humidity of 60–70%, and light and dark time of 12 h. PANC-1 cells transfected with NC shRNA and PANC-1 cells transfected with FOSL1 shRNA (1×10^7 cells/ml) were injected into the right flank of each mouse. After the average volume (mm^3) of xenograft tumors in NC KD group reaching to 150 mm^3, tumor volume and mice weight were recorded. After 32 days of feeding and observation, the mice were killed to detect the weight of tumors in each group. Tumor volume was recorded every three days. Tumor volume was measured with a vernier caliper and calculated using the formula, $(ab^2)/2$, where a and b represent length and width of the tumor.

H&E staining

The lung, liver, heart, kidney and spleen tissue samples of xenograft model mice were fixed with 4% paraformaldehyde, dehydrated with ethanol, immersed in xylene, embedded in paraffin wax and sectioned into 4.0 μm slides. The paraffin-embedded sections were stained with H&E according to the manufacturer's instructions (Beyotime, Shanghai, China). Each group of samples was observed with a DM6B positive fluorescence microscope (Leica, Frankfurt, Germany). Five images were randomly captured per slide.

Immunohistochemical (IHC) staining

Xenograft tumors were embedded in paraffin wax and sectioned in slides. Sections were incubated with 0.3% hydrogen peroxide for 20 min to quench endogenous peroxidase and then incubated with 1.0% BSA for 30 min to block. After blocking, the paraffin-embedded section was incubated with anti-Ki67 primary antibody at 4 °C for 12 h, incubated with secondary antibody for another 1.0 h at room temperature and then counterstained for 1 min with hematoxylin. Each group was examined using the DM6B positive fluorescence microscope (Leica, Frankfurt, Germany). Five images were randomly captured per slide.

Statistical analysis

The data were analyzed using SPSS 19.0. The results are expressed as means ± SD. Differences between treatment regimens were analyzed by two-tailed Student's *t*-test or one-way ANOVA. $P < 0.05$ was considered statistical significance.

Results

FOSL1 promotes the malignant progression of pancreatic cancers

The transcription factor FOSL1 is involved in regulating multiple molecular events to promote the progression of various cancers [10–13]. To evaluate whether FOSL1 is a valuable target for pancreatic cancer treatment, we analyzed the differential expression of FOSL1 in cancer tissues and adjacent normal tissues of 31 cancers from TCGA (Fig. 1A and B, Supplementary Fig. 1A and B). FOSL1 was generally overexpressed in various types of cancer, including pancreatic adenocarcinoma (PAAD) (Fig. 1A, Supplementary Fig. 1A and B). The expression level of FOSL1 was high in all stages of pancreatic cancer (Fig. 1B). Further study on the relationship between FOSL1 expression and patient survival showed that with

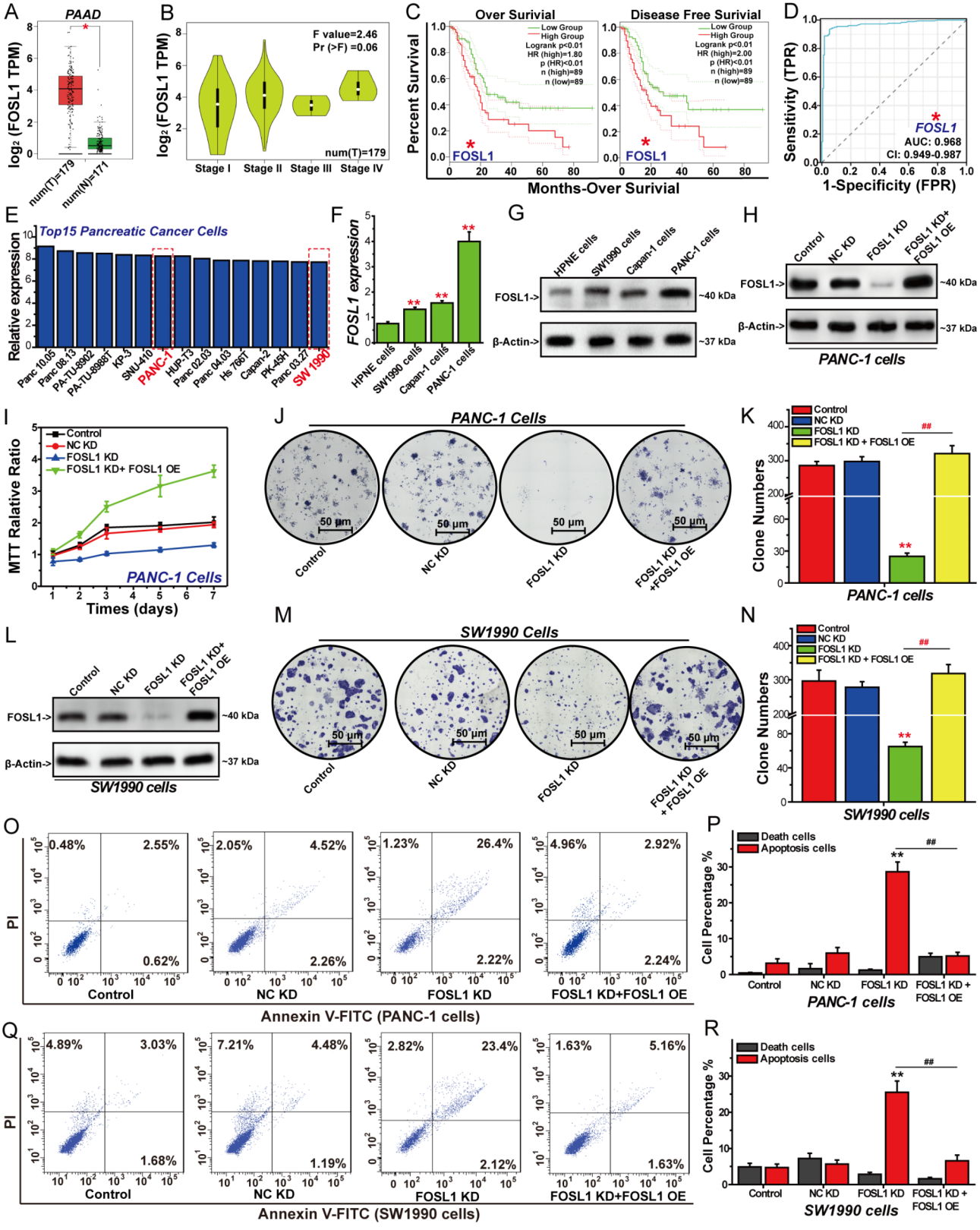

Fig. 1 (See legend on next page.)

(See figure on previous page.)

Fig. 1 FOSL1 promotes the proliferation of pancreatic cancer cells in vitro. (**A**) Differential expression of FOSL1 between PAAD tissues and adjacent tissues in TCGA project. (**B**) Pathological stage plot for the expression of FOSL1 in pancreatic cancer. (**C**) ROC curves for the relationship of FOSL1 expression and the prognosis of patient with pancreatic cancer. (**D**) The correlation between FOSL1 expression and the survival of patient with pancreatic cancers. (**E**) Distribution of FOSL1 mRNA expression in different pancreatic cancer cell lines. (**F**) Q-PCR analysis of the distribution of FOSL1 mRNA expression in SW1990 cells, Capan-1 cells and PANC-1 cells. (**G**) Western blots analysis of the expression of FOSL1 in SW1990 cells, Capan-1 cells and PANC-1 cells. (**H**) Western blots analysis of FOSL1 expression in PANC-1 cells. (**I**) Relative viability of PANC-1 cells in each group analyzed by MTT assay. (**J**) Effects of FOSL1 on the formation of PANC-1 clones. (**K**) Number of PANC-1 clones in each group. (**L**) Western blots analysis of FOSL1 expression in SW1990 cells. (**M**) Effects of FOSL1 on the formation of SW1990 clones. (**N**) Number of SW1990 clones in each group. (**O**) Effects of FOSL1 on the apoptosis of PANC-1 cells. (**P**) Percentage of PANC-1 apoptosis cells. (**Q**) Effects of FOSL1 on the apoptosis of SW1990 cells. (**R**) Percentage of SW1990 apoptosis cells. The results from three independent experiments were statistically analyzed using one way ANOVA: $^{*}P<0.05$, $^{**}P<0.01$ compared with control group, $^{\#}P<0.05$, $^{\#\#}P<0.01$ compared with FOSL1 KD group. Images were selected randomly from 5 images

the increase of FOSL1 expression, the overall survival (OV) and disease free survival (RFS) of pancreatic cancer patient were significantly reduced (Fig. 1C, Supplementary Fig. 1C). Subsequently, effects of FOSL1 expression on prognosis of pancreatic cancer was analyzed using ROS curve. AUC value of ROC curve is indicative of the correlation between target gene expression and the prognosis of cancers. The AUC value of the ROC curve of FOSL1 is 0.97, indicating that the expression of FOSL1 was significantly associated with poor prognosis of pancreatic cancer (Fig. 1D). The expression distribution of FOSL1 mRNA in different pancreatic cancer cell lines indicated that the expression level of FOSL1 was high in PANC-1 cells and SW1990 cells (Fig. 1E). Q-PCR and Western blots results confirmed that the expression of FOSL1 in pancreatic cancer cells was higher than that in normal pancreatic cells. The expression level of FOSL1 was high in PANC-1 cells and SW1990 cells (Fig. 1F, G). Therefore, we selected PANC-1 cells and SW1990 cells for further study.

Knockdown of FOSL1 inhibits the proliferation of pancreatic cancer cells in vitro and in vivo

We firstly investigated the effects of FOSL1 on the proliferation of PANC-1 cells at different time by MTT assay and colony formation assay (Fig. 1H-N). FOSL1 shRNA caused a significant decrease in FOSL1 expression, and FOSL1 cRNA reversed the inhibition of FOSL1 expression in PANC-1 cells (Fig. 1H). Knockdown of FOSL1 significantly inhibited the proliferation of PANC-1 cells and the formation of PANC-1 clones. The inhibitory effect of silencing FOSL1 on PANC-1 cell proliferation was reversed by overexpression of FOSL1 (Fig. 1I-K). FOSL1 shRNA also caused a significant decrease in FOSL1 expression, and FOSL1 cRNA reversed the inhibition of FOSL1 expression in SW1990 cells (Fig. 1L). Compared with control group or NC KD group, the number of SW1990 clones in FOSL1 knockdown (FOSL1 KD) group was significantly reduced. Overexpression of FOSL1 reversed the inhibitory effect of silencing FOSL1 on the proliferation of SW1990 cells, where the number of clones in the FOSL1 KD with FOSL1 overexpression (FOSL1 OE) group was significantly increased compared with the FOSL1 KD group (Fig. 1M and N). Similarly, knockdown of FOSL1 promoted the apoptosis of PANC-1 cells and SW1990 cells, and this inhibitory effect was significantly reversed by overexpression of FOSL1 (Fig. 1O-R). Subsequently, we constructed stable FOSL1-knockdown PANC-1 cells and evaluated the effect of FOSL1 on the growth of pancreatic cancer cells in vivo (Fig. 2). We used FOSL1-knockdown PANC-1 cells and NC-knockdown PANC-1 cells to construct the cell line-derived xenograft (CDX) tumors (Fig. 2A). After 32 days of observation, knockdown of FOSL1 did not cause significant damage of the kidney, Lung, Spleen, Liver and Heart of mice (Fig. 2B). Meanwhile, knockdown of FOSL1 had no effect on the body weight of mice (Fig. 2C). However, knockdown of FOSL1 significantly inhibited the volume and weight of PANC-1 CDX tumors (Fig. 2D-F). Compare with NC KD group, the inhibition ratio of tumor volume and weight in FOSL1 KD group were 49.19% and 56.18%, respectively (Fig. 2G). The IHC results of Ki-67 in FOSL1 KD group were significantly decreased, which confirmed that knockdown of FOSL1 could significantly inhibit the progression of PANC-1 xenograft tumors (Fig. 2H and I).

FOSL1 regulates genes-involved in cell stemness, EMT and multidrug efflux system

To clarify the mechanism of FOSL1 in regulating the proliferation of pancreatic cancer cells, we used RNA sequencing to analyze the effects of FOSL1 on the expression of genes in PANC-1 cells (Fig. 3A-C, Supplementary Table 1). Knockdown of FOSL1 induced up-regulation of 2145 DEGs and down-regulation of 305 DEGs in PANC-1 cells. The results of GO functional enrichment and KEGG pathways enrichment showed that DEGs regulated by FOSL1 were mostly associated with cell stemness, epithelial-mesenchymal transition (EMT) and multidrug efflux system (Fig. 3A and B, Supplementary Table 2). By comparation of NC KD group vs. FOSL1 KD group, 10 DEGs were selected based on the results of GO enrichment and KEGG pathway enrichment (Fig. 3C). Among these DEGs, 3 genes were associated with cells stemness, 4 genes were associated with cell invasion and migration, 3 genes were involved in multidrug efflux

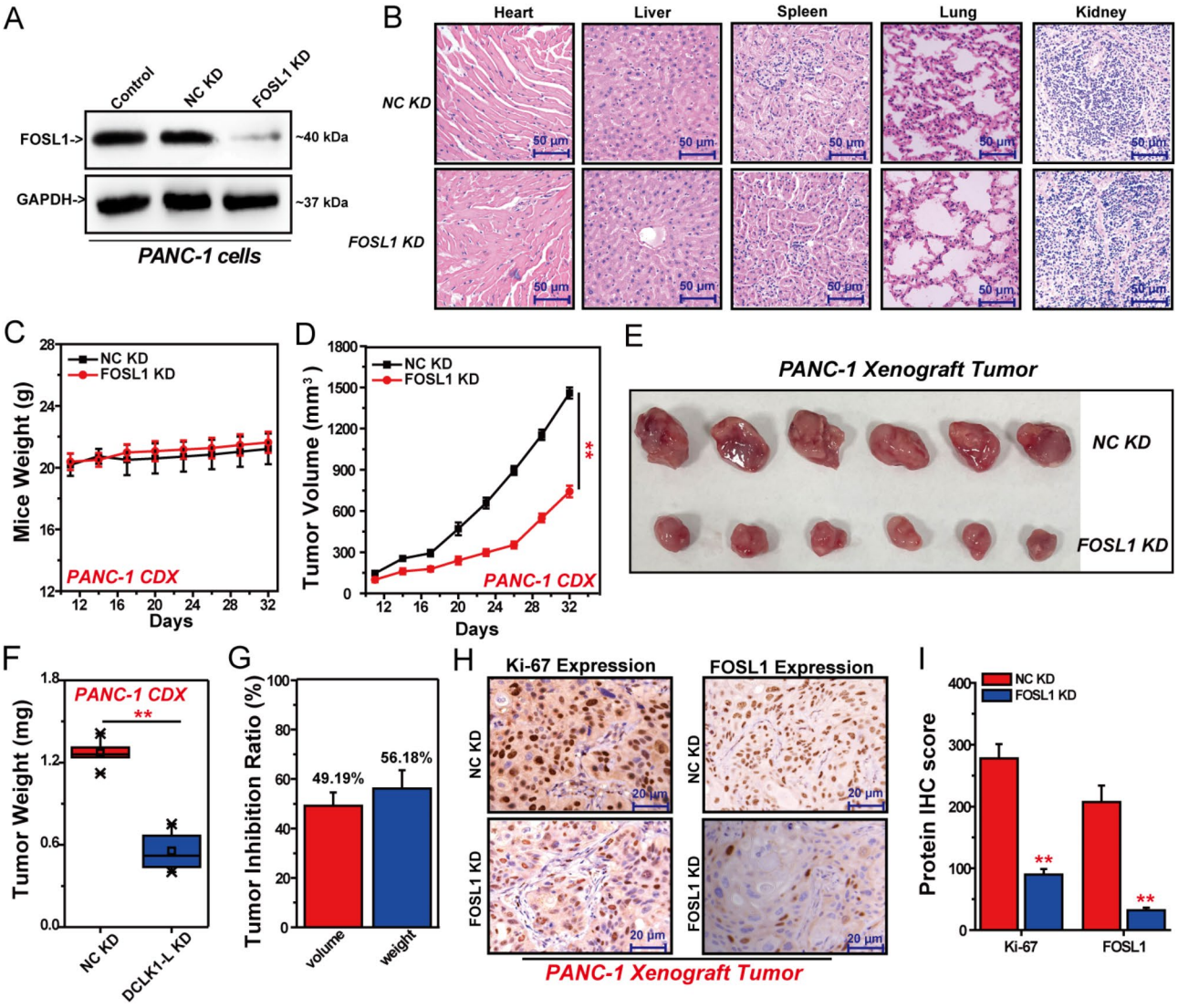

Fig. 2 Knockdown of FOSL1 inhibits the proliferation of PANC-1 xenograft tumors. (**A**) Western blots analysis of FOSL1 expression in PANC-1 cells. (**B**) Tissue damage was determined by H&E staining. (**C**) Mice weight of PANC-1 xenograft tumor model. (**D**) Effects of FOSL1 on tumor volume. (**E**) The photos of tumors in each group. (**F**) Effects of FOSL1 on tumor weight. (**G**) The inhibition ratio of FOSL1 on the volume and weight of PANC-1 xenograft tumors. (**H**) The expression of Ki-67 in each group analyzed by IHC. (**I**) IHC scores of Ki-67 and FOSL1 in each group. The results from three independent experiments were statistically analyzed using one way ANOVA: $^{*}P < 0.05$, $^{**}P < 0.01$ compared with NC KD group. Images were selected randomly from 5 images

system. The differential expression of these genes in pancreatic cancer tissues and adjacent normal tissues indicated that all genes except CD44 were overexpressed in pancreatic cancer (Fig. 3D). Further bioinformatic analysis showed that the expressions of CD44, HMGA1 and cadherin 1 (CDH1) were positively correlated with the expression of FOSL1 in pancreatic cancer cells (Fig. 4A). The AUC values of the ROC curves for BMI1, HMGA1, vimentin (VIM), β-catenin (CTNNB1), matrix metallopeptidase 1 (MMP1), CDH1, ATP binding cassette subfamily B member 1 (ABCB1), ATP binding cassette subfamily G member 1 (ABCG1) and ATP binding cassette subfamily C member 4 (ABCC4) were all greater than 0.90, indicating that the expression of these genes was significantly associated with the poor prognosis of pancreatic cancer (Fig. 4B). Survival analysis suggested that with the increase of CD44, HMGA1 and MMP1 expression, the OV of pancreatic cancer patient was significantly reduced, while with the increase of ABCB1expression, the OV was significantly increased (Fig. 4C). In summary, HMGA1 is the key overexpressed gene in pancreatic cancer, which is positively correlated with FOSL1 expression and is related to the malignant progression and poor prognosis of pancreatic cancer.

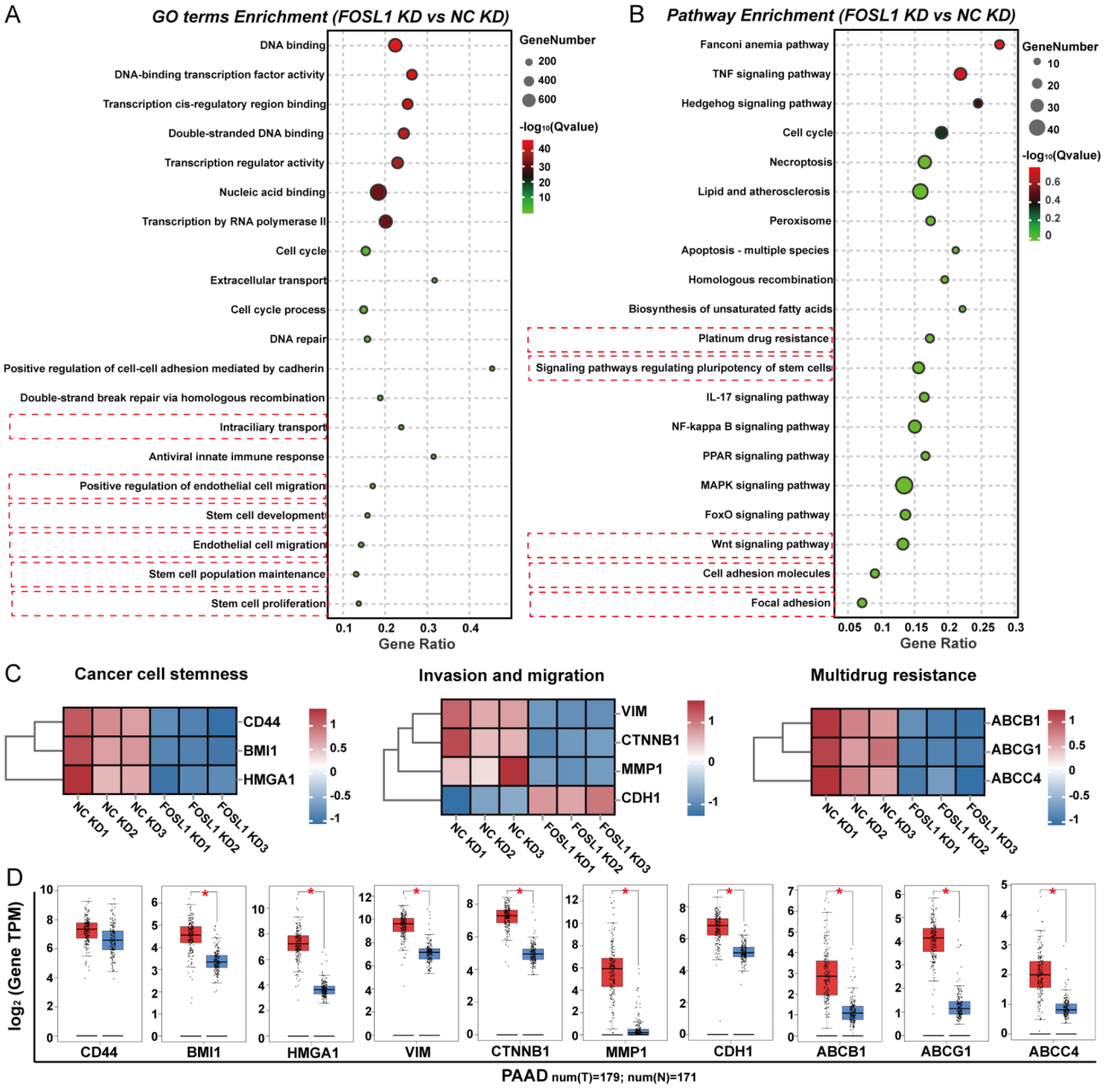

Fig. 3 FOSL1 regulated genes-involved in cell stemness, EMT and multidrug efflux system. (**A**) GO enrichment and (**B**) KEGG pathway enrichment analysis of DEGs regulated by FOSL1. (**C**) Heatmap plot for the DEGs involved in cell stemness, invasion and migration, and multidrug efflux system analyzed by RNA sequencing. (**D**) Differential expression of genes between cancer tissues and adjacent tissues of pancreatic cancers in TCGA project. Data were statistically analyzed using one way ANOVA: $^{*}P < 0.05$ compared with adjacent tissues

Knockdown of FOSL1 inhibits stemness, invasion and migration, and multidrug efflux system

Sphere formation assay is used to assess the stemness of cancer cells [35]. More three-dimensional spheres indicate that the proliferation ability and stemness of cancer cells are stronger [35]. Compared with control group and NC KD group, the number of PANC-1 spheres and SW1990 spheres was significantly reduced in FOSL1 KD group (Fig. 5A and B). Effects of FOSL1 on the formation of spheres suggests that FOSL1 promoting the stemness of pancreatic cancer cells. Subsequently, we analyzed the effects of FOSL1 on the expression of CD44, a biomarker of stem cell. The results of IF showed that knockdown of FOSL1 inhibited the expression of CD44. Compared with control group and NC KD group, the red fluorescence intensity corresponding to CD44 was significantly reduced in FOSL1 KD group (Fig. 5C). Further Western blots results confirmed that knockdown of FOSL1

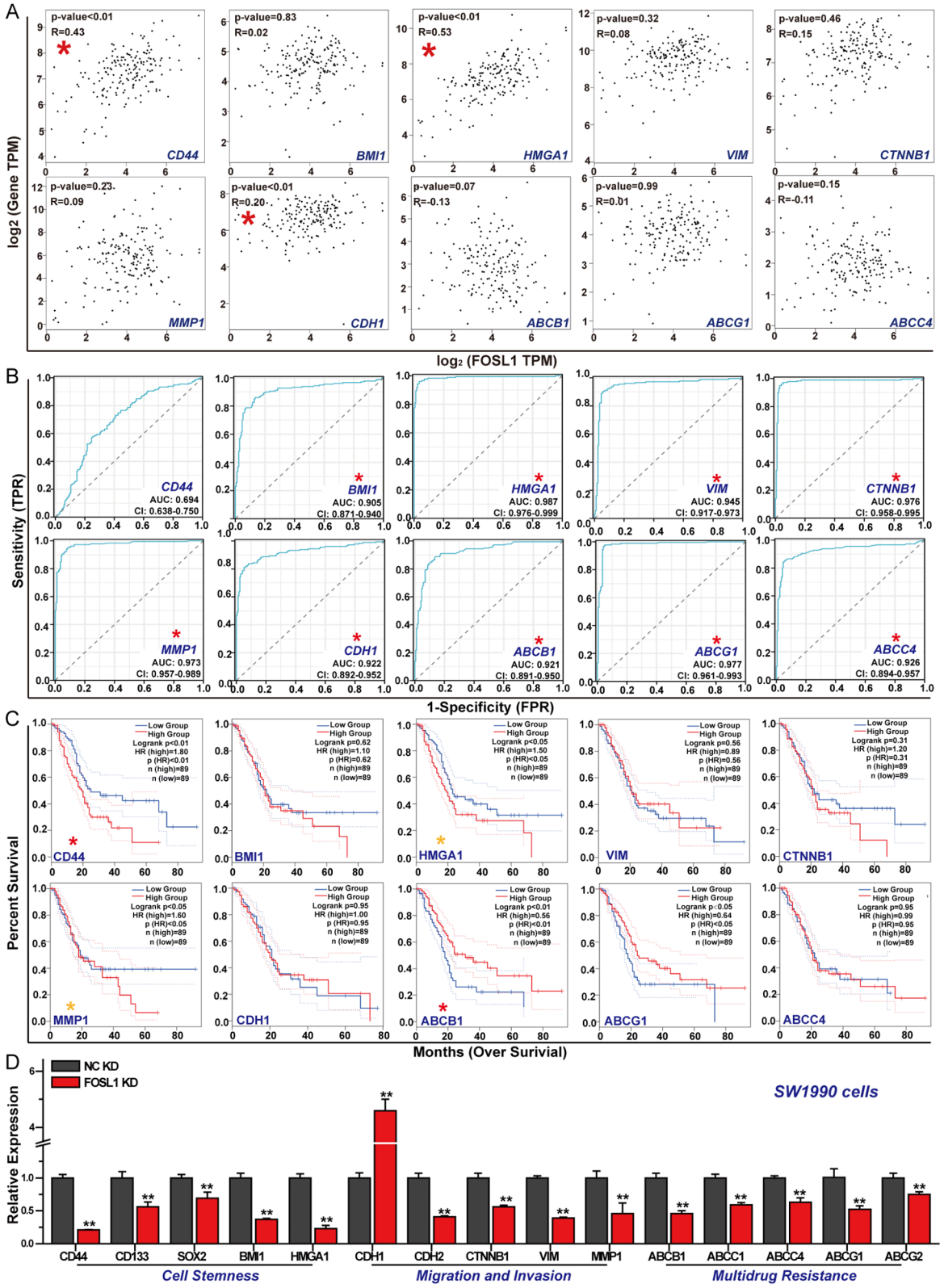

Fig. 4 Effects of FOSL1-reguated genes in the progression of pancreatic cancers. (**A**) Correlation analysis of FOSL1 expression and target genes expression in PAAD. (**B**) ROC curves for the relationship of key genes expression and the survival of patient with PAAD. (**C**) The relationship between key genes expression and overall survival of patient with PAAD. (**D**) Effects of FOSL1 on the expression of key genes analyzed by Q-PCR. The results from three independent experiments were statistically analyzed using one way ANOVA: $^{*}P < 0.05$, $^{**}P < 0.01$ compared with NC KD group

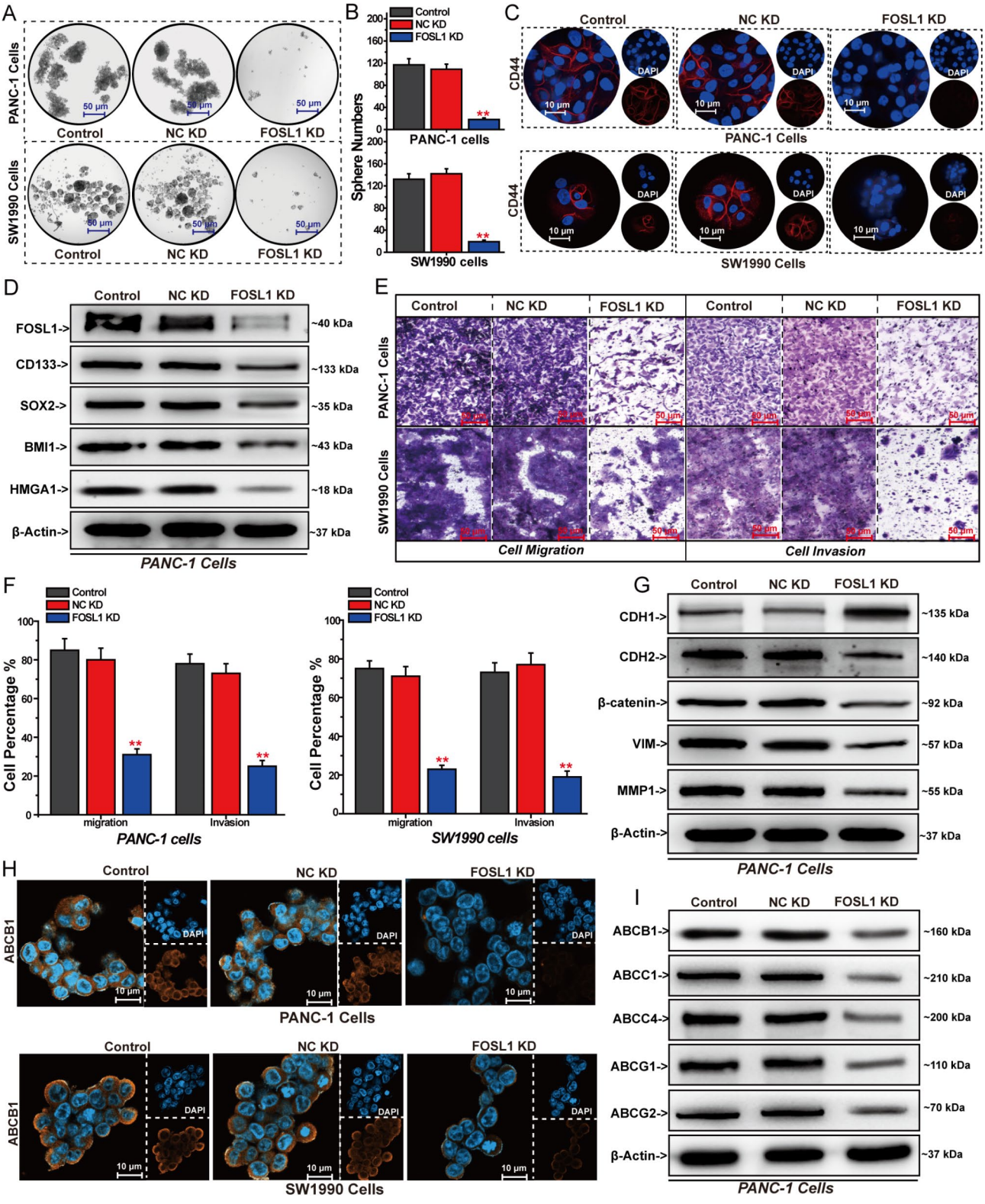

Fig. 5 (See legend on next page.)

(See figure on previous page.)

Fig. 5 Effects of FOSL1 on cell stemness, invasion and migration, and multidrug efflux system. (**A**) Effects of FOSL1 on the formation of three-dimensional spheres. (**B**) Sphere numbers in PANC-1 cells and SW1900 cells. (**C**) Effects of FOSL1 on CD44 expression analyzed by immunofluorescence. (**D**) Effects of FOSL1 on stemness-related genes expression in PANC-1 cells analyzed by Western blots. (**E**) Effects of FOSL1 on the invasion and migration of pancreatic cells. (**F**) Percentage of migrated cells and invaded cells in SW1990 cells and PANC-1 cells. (**G**) Effects of FOSL1 on metastasis-related genes expression in PANC-1 cells analyzed by Western blots. (**H**) Effects of FOSL1 on ABCB1 expression analyzed by immunofluorescence. (**I**) Effects of FOSL1 on the expression of genes related to multidrug efflux system in PANC-1 cells analyzed by Western blots. Images were selected randomly from 5 images. The results from three independent experiments were statistically analyzed using one way ANOVA: $^{*}P < 0.05$, $^{**}P < 0.01$ compared with control group

significantly inhibited the expression of CD133, SOX2, BMI1 and HGMA1, which regulate the stemness of cancer cell (Fig. 5D). Meanwhile, we investigated the effects of FOSL1 on the invasion and migration of pancreatic cancer cells. Knockdown of FOSL1 significantly inhibited the invasion and migration of both PANC-1 cells and SW1990 cells (Fig. 5E and F). Western blots results showed that knockdown of FOSL1 significantly inhibited the expression of CDH2, CTNNB1, VIM and MMP1, and promoted the expression of CDH1, which regulate cancer cell metastasis (Fig. 5G). We also investigated the effects of FOSL1 on the expression of genes in regulating multidrug efflux system using IF and Western blots. Silencing FOSL1 expression significantly decreased the expression of ABCB1, ATP binding cassette subfamily C member 1 (ABCC1), ABCC4, ABCG1 and ATP binding cassette subfamily G member 2 (ABCG2) in pancreatic cancer cells (Fig. 5H and I).

FOSL1 regulates HMGA1 expression to promote the proliferation of pancreatic cancer cells

We used co-IP Mass spectrometry to analyze the proteome interacting with FOSL1 in PANC-1 cells. 810 proteins were detected to potentially interact with FOSL1. 70 common genes were detected by RNA sequencing and FOSL1 co-IP Mass spectrometry (Fig. 6A, Supplementary Table 3). The results of GO functional enrichment and KEGG pathways enrichment showed that these 70 genes were involved in regulating DNA packaging, DNA repair, cell apoptosis, cell necroptosis, cell metastasis and immune response (Fig. 6B and C). Among these genes, HMGA1 may be a key target regulated by FOSL1 and act synergistically with FOSL1. Similar to FOSL1, HMGA1 was also highly expressed in SW1990 cells and PANC-1 cells (Fig. 6D and E). Co-IP assay confirmed that FOSL1 directly interacted with HMGA1 in PANC-1 cells (Fig. 6F). Subsequently, we investigated the regulatory relationship between FOSL1 and HMGA1 in SW1990 cells by Q-PCR and Western blots. The resulted showed that knockdown of FOSL1 significantly inhibited the expression of HMGA1, while knockdown of HMGA1 did not significantly affect the expression of FOSL1 (Fig. 6G). This suggest that HMGA1 is the downstream target of FOSL1. As an important transcription factor, FOSL1 can regulate the expression of downstream target genes at the transcriptional level. To analyze whether HMGA1 is a downstream target directly regulated by FOSL1 at the transcriptional level, we analyzed ChIP-seq of FOSL1 using Cistrome Data Browser. From the ChIP-seq data of FOSL1, we can clearly observe the peak of HMGA1, which means that HMGA1 is directly regulated by FOSL1 at the transcriptional level (Fig. 6H, Supplementary Fig. 2). Q-PCR of ChIP confirmed that the promoter of HMGA1 directly binds to FOSL1 (Fig. 6I).

HMGA1 reverses the inhibitory effect of FOSL1 knockdown on malignant proliferation of pancreatic cancer cells

As a direct downstream target of FOSL1, overexpression of HMGA1 promoted the expression of FOSL1 in SW1990 cells (Fig. 7A). We firstly investigated the effects of HMGA1 on the proliferation of SW1990 cells at different time by MTT assay (Fig. 7B). Knockdown of HMGA1 significantly inhibited the proliferation of SW1990 cells. Compared with control group or NC KD group, the cell viability of SW1990 cells were significantly inhibited. The results of colony formation assay showed that the number of SW1990 clones in FOSL1 KD group was significantly reduced. Overexpression of HMGA1 reversed the inhibitory effect of silencing FOSL1 on the formation of SW1990 clones, where the number of clones in the FOSL1 KD with HMGA1 OE group was significantly increased compared with the FOSL1 KD group (Fig. 7C and D). Moreover, Knockdown of FOSL1 promoted the apoptosis of SW1990 cells, and this inhibitory effect was significantly reversed by overexpression of HMGA1 (Fig. 7E and F). The percentage of apoptosis SW1990 cells increased from 7.18% in NC KD group to 40.6% in FOSL1 KD group, and the percentage of apoptosis cells decreased to 5.37% in in FOSL1 KD with HMGA1 OE group. Subsequently, we analyzed the effects of HMGA1 on the proliferation of PANC-1 cells (Fig. 7G and H). The results of MTT assay confirmed that knockdown of HMGA1 inhibited the proliferation of PANC-1 cells (Fig. 7H). The inhibitory effect of silencingFOSL1 on the formation of PANC-1 clones was reversed by overexpression of HMGA1 (Fig. 7I and J). Knockdown of FOSL1 promoted the apoptosis of PANC-1 cells, and this inhibitory effect was significantly reversed by overexpression of HMGA1 (Fig. 7K and L). HMGA1 is the key target of FOSL1 that promotes malignant proliferation of pancreatic cancer cells.

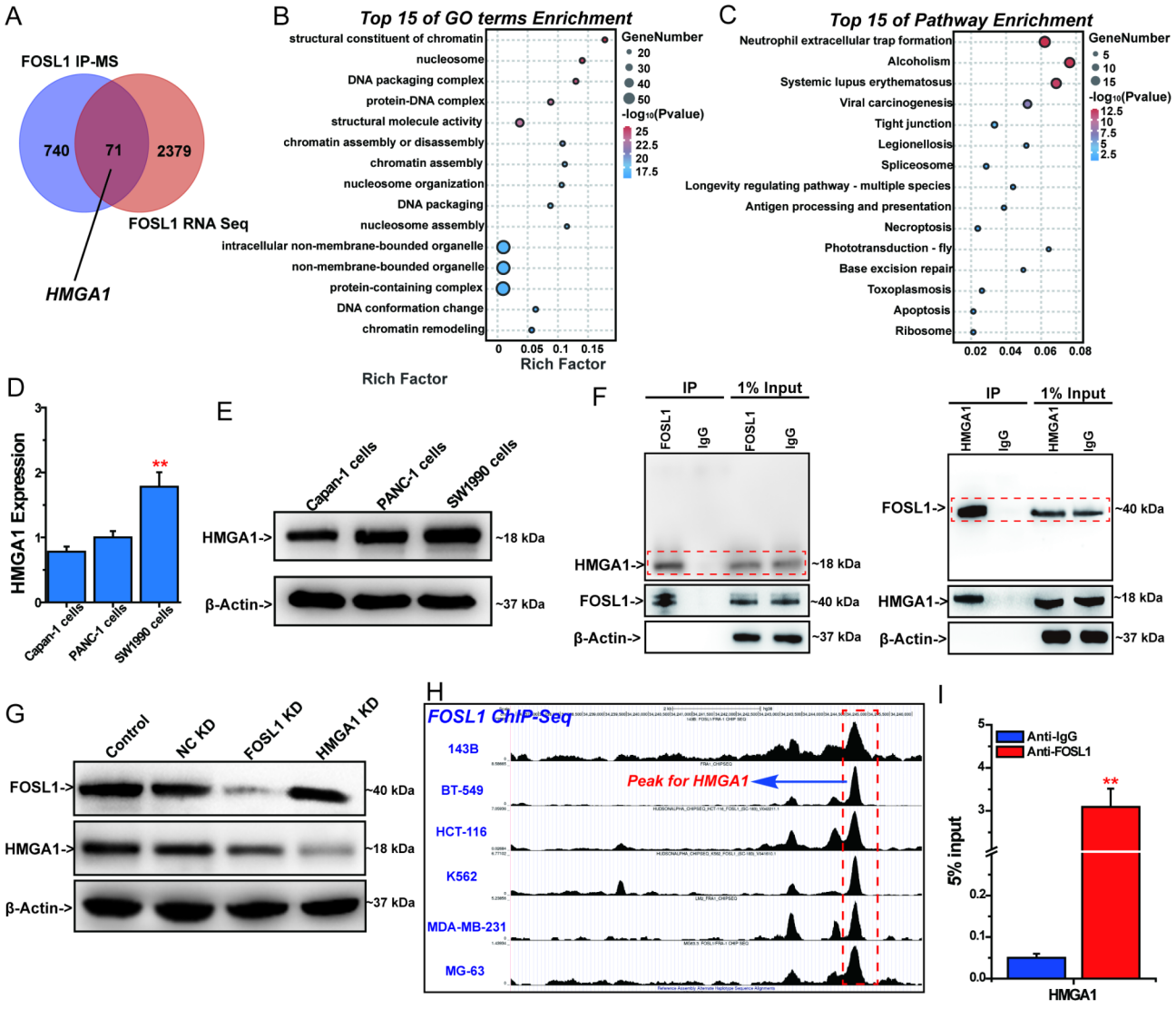

Fig. 6 The relationship between FOSL1 and HMGA1. (**A**) Venn diagrams for common genes detected in RNA sequencing and FOSL1 co-IP Mass spectrometry. (**B**) CO enrichment of common genes. (**C**) KEGG pathway enrichment of common genes. (**D**) HMGA1 expression in different pancreatic cancer cells analyzed by Q-PCR. (**E**) Western blots analysis of the expression of FOSL1 in different pancreatic cancer cells. (**F**) Co-IP analysis of the interaction between FOSL1 and HMGA1 in PANC-1 cells. (**G**) The regulatory relationship between FOSL1 and HMGA1 in SW1990 cells analyzed by Western blots. (**H**) The regulation of FOSL1 on HMGA1 in ChIP-seq data of FOSL1. (**I**) The accumulation of HMGA1 was analzed by Q-PCR of ChIP. The results from three independent experiments were statistically analyzed using one way ANOVA: $^{*}P < 0.05$, $^{**}P < 0.01$ compared with anti-IgG group

Knockdown of HMGA1 inhibits stemness, invasion and migration, and multidrug efflux system

Knockdown of HMGA1 significantly inhibited the formation of three-dimensional spheres (Fig. 8A and B). IF results confirmed that knockdown of HMGA1 inhibited the expression of CD44, where the red fluorescence intensity significantly decreased in the HMGA1 KD group (Fig. 8C). Meanwhile, the expression of CD133, BMI1, snail family transcriptional repressor 1 (SNAIL1) and POU class 5 homeobox 1 (OCT4) were significantly decreased after HMGA1 knockdown in SW1990 cells and PANC-1 cells (Fig. 8D and E). Effects of HMGA1 on the invasion and migration of pancreatic cancer cells were also investigated. Knockdown of HMGA1 significantly inhibited the invasion and migration of both PANC-1 cells and SW1990 cells (Fig. 8F and G). Q-PCR and Western blots results showed that the expressions of CDH2, CTNNB1, VIM and MMP1 were significantly decreased, while the expression of CDH1 was significantly increased after HMGA1 knockdown in SW1990 cells and PANC-1 cells (Fig. 8H and I). We also investigated the effects of HMGA1 on the expression of genes-related to multidrug efflux system using Q-PCR and Western blots. Silencing HMGA1 expression significantly inhibited the expression of ABCB1, ABCC1, ABCC4, ABCG1 and ABCG2 in SW1990 cells and PANC-1 cells (Fig. 8J and K). HMGA1

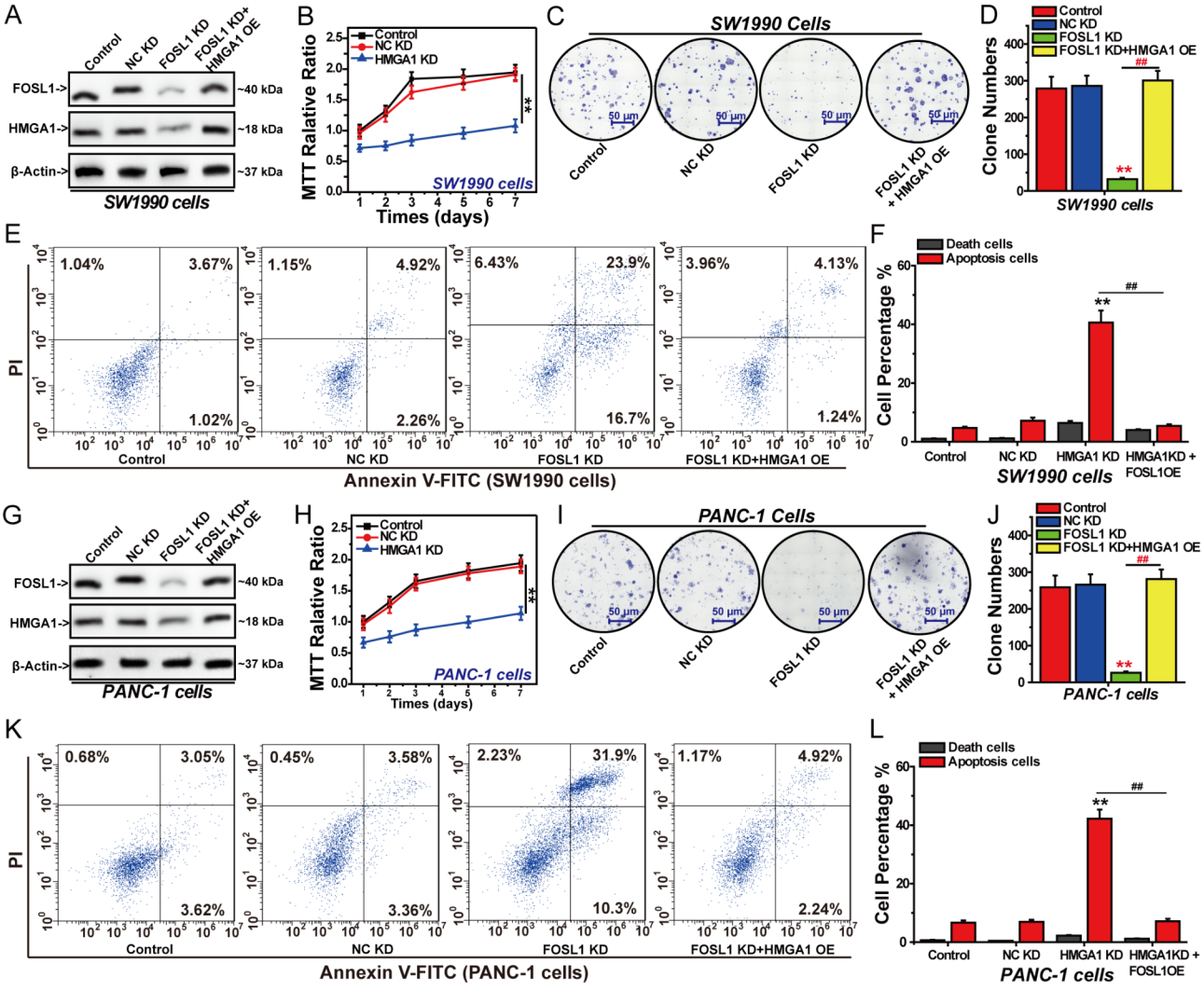

Fig. 7 Effects of HMGA1 on the inhibitory effect of FOSL1 knockdown on the proliferation of pancreatic cells in vitro. (**A**) Expression of FOSL1 and HMGA1 in SW1990 cells analyzed by Western blots. (**B**) Effects of HMGA1 on the viability of SW1990 cells. (**C**) Effects of HMGA1 and FOSL1 on the formation of SW1990 clones. (**D**) Number of SW1990 clones in each group. (**E**) Effects of HMGA1 and FOSL1 on the apoptosis of SW1990 cells. (**F**) Percentage of apoptosis of SW1990 cells. (**G**) Expression of FOSL1 and HMGA1 in PANC-1 cells analyzed by Western blots. (**H**) Effects of HMGA1 on the viability of PANC-1 cells. (**I**) Effects of HMGA1 and FOSL1 on the formation of PANC-1 clones. (**J**) Number of PANC-1 clones in each group. (**K**) Effects of HMGA1 and FOSL1 on the apoptosis of PANC-1 cells. (**L**) Percentage of apoptosis of PANC-1 cells. The results from three independent experiments were statistically analyzed using one way ANOVA: $^{*}P<0.05$, $^{**}P<0.01$ compared with control group, $^{*}P<0.05$, $^{**}P<0.01$ compared with control group, $^{\#}P<0.05$, $^{\#\#}P<0.01$ compared with HMGA1 KD group

promotes the malignant progression of pancreatic cancer by regulating cancer cells stemness, invasion and migration, and multidrug efflux system.

Targeted Inhibition of FOSL1 and HMGA1 expression significantly inhibit the proliferation of pancreatic cancer cells

We simultaneously knocked down the expression of FOSL1 and HMGA1 to investigate their combined effects on the proliferation of pancreatic cancer cells. FOSL1 shRNA significantly decreased the expression of FOSL1 and HMGA1, HMGA1 shRNA significantly decreased the expression of HMGA1, and FOSL1 shRNA combined with HMGA1 shRNA significantly decreased the expression of FOSL1 and HMGA1 in PANC-1 cells (Fig. 9A). Compared with FOSL1 KD group or HMGA1 KD group, the number of PANC-1 clones was significantly reduced in FOSL1 KD with HMGA1 KD group (Fig. 9B and C). Meanwhile, FOSL1 shRNA combined with HMGA1 shRNA significantly decreased the expression of FOSL1 and HMGA1 in SW1990 cells (Fig. 9D). Simultaneous knockdown of FOSL1 and HMGA1 significantly inhibited the formation of SW1990 clones (Fig. 9E and F). Moreover, simultaneous knockdown of FOSL1 and HMGA1 significantly promoted the apoptosis of PANC-1 cells. The percentage of apoptosis cells increased from

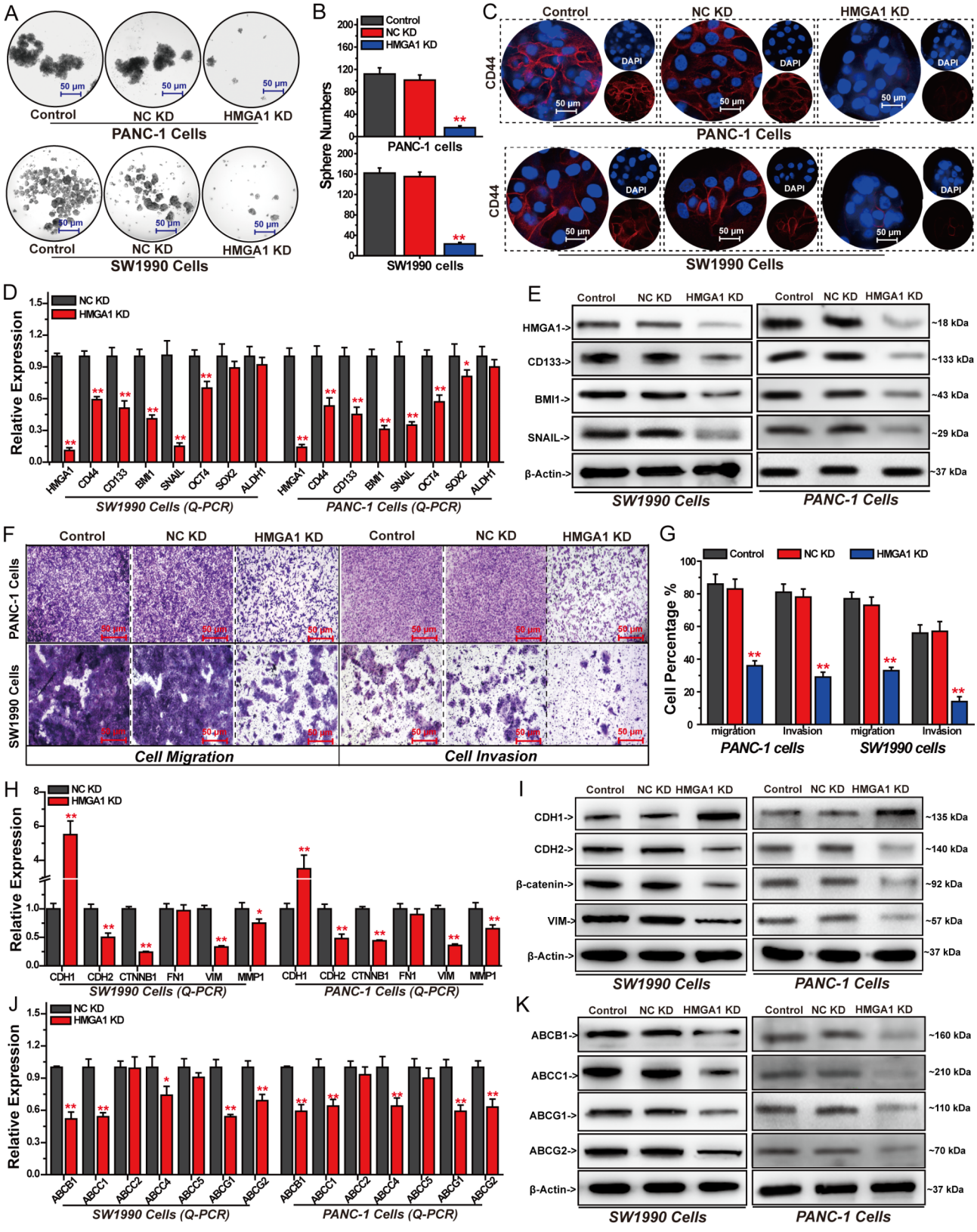

Fig. 8 (See legend on next page.)

(See figure on previous page.)

Fig. 8 Effects of HMGA1 on cell stemness, invasion and migration, and multidrug efflux system. (**A**) Effects of HMGA1 on the formation of three-dimensional spheres. (**B**) Sphere numbers in PANC-1 cells and SW1900 cells. (**C**) Effects of HMGA1 on CD44 expression in PANC-1 cells and SW1990 cells analyzed by immunofluorescence. (**D**) Effects of HMGA1 on stemness-related genes expression in SW1990 cells and in PANC-1 cells analyzed by Q-PCR. (**E**) The expression of stemness-related genes in SW1990 cells and PANC-1 cells analyzed by Western blots. (**F**) Effects of HMGA1 on the invasion and migration of pancreatic cells. (**G**) Percentage of migrated cells and invaded cells in SW1990 cells and PANC-1 cells. (**H**) Effects of HMGA1 on EMT-related genes expression in SW1990 cells and in PANC-1 cells analyzed by Q-PCR. (**I**) The expression of EMT-related genes in SW1990 cells and PANC-1 cells analyzed by Western blots. (**J**) Effects of HMGA1 on the expression of genes related to multidrug efflux system in SW1990 cells and in PANC-1 cells analyzed by Q-PCR. (**K**) The expression of genes related to multidrug efflux system in SW1990 cells and PANC-1 cells analyzed by Western blots. The results from three independent experiments were statistically analyzed using one way ANOVA: $^{*}P<0.05$, $^{**}P<0.01$ compared with control group. Images were selected randomly from 5 images

23.5% in FOSL1 KD group and 26.5% in HMGA1 KD group to 55.7% in FOSL1 KD with HMGA1 KD group (Fig. 9G and H). The simultaneous knockdown of FOSL1 and HMGA1 was also significant in promoting apoptosis of SW1990 cells. The percentage of apoptosis cells increased from 28.8% in FOSL1 KD group and 30.5% in HMGA1 KD group to 49.5% in FOSL1 KD with HMGA1 KD group (Fig. 9I and J). In summary, targeted inhibition of FOSL1 and HMGA1 expression significantly inhibit the proliferation of pancreatic cancer cells.

Discussion

Novel therapeutic strategies are urgently required for the treatment of challenging pancreatic cancer, one of the leading causes for cancer-related death worldwide [1–3]. With the development of sequencing technology and bioinformatics, innovative targeted therapy has the potential to improve survival and quality of life for patients with pancreatic cancer [6–9]. The success of PARP targeted therapy and KRAS targeted therapy demonstrates that targeted therapy is another option and hope for the treatment of advanced and metastatic pancreatic cancer [7–9]. However, existing targeted drugs have limitations such as narrow clinical indications and drug resistance [6–9]. Novel targets and therapeutic strategies are urgently required for the treatment of challenging pancreatic cancer. FOSL1 is overexpressed in many human cancers and contributes to malignant progression and poor prognosis [13–19]. Targeting FOSL1 in monotherapy or combination therapy may have good therapeutic effect on challenging pancreatic cancer. Herein, we investigated the effect FOSL1 on the malignant proliferation of pancreatic cancer cells and the corresponding mechanism.

Transcription factor FOSL1 has been shown to promote the malignant proliferation and poor prognosis in a variety of cancers and is associated with chemotherapy resistance [13–17]. We found that FOSL1 was overexpressed in pancreatic cancer cells. The results of survival analysis and prognosis analysis showed that with the increase of FOSL1 expression, the survival and prognosis of pancreatic cancer patients became worse. Knockdown of FOSL1 inhibited the proliferation of pancreatic cancer cells in vitro and in vivo. RNA sequencing studies showed that FOSL1 promoted pancreatic cancer progression by regulating cancer cell stemness, metastasis, and multidrug efflux system. Further mechanism studies showed that silencing FOSL1 expression inhibited the formation of three-dimensional spheres and the expression of CD44, BMI1 and HMGA1. Sphere formation assay is used to assess the stemness of cancer cells [35]. More three-dimensional spheres indicate that the proliferation ability and stemness of cancer cells are stronger [35]. CD44 is an important stem cell biomarker that is associated with the stemness of cancer cells [36]. BMI1 and HMGA1 paly crucial roles of cancer stemness including invasion, drug resistance and cancer initiation [37, 38]. The effect of FOSL1 on the formation of three-dimensional spheres and the expression of these genes confirmed that FOSL1 promoted the stemness of pancreatic cancer cells. In fact, FOSL1 has been shown to induce the stemness of pancreatic cancer cells by regulating RNA polymerase II-associated factor expression [39]. FOSL1 promotes the stemness of hepatocellular carcinoma cells by regulating HEY1 expression [40]. FOSL1 promotes stem cell-like characteristics and facilitates metastasis in osteosarcoma by targeting SOX2 [41]. FOSL1 promotes colorectal cancer stem-like properties by targeting Nanog homeobox [42]. Stemness of cancer cells has been shown to promote cancer invasion and drug resistance, and is closely related to the malignant proliferation and poor prognosis of cancers [43]. Indeed, FOSL1 regulated the expression of genes involved in regulating EMT and multidrug efflux system. EMT is a complex physiological process whose dysfunction can promote invasion and metastasis of cancer [44]. Decreased expression of epithelial markers CDH1 and elevated expression of VIM and CDH2 have been shown to contribute to the invasion and metastasis of cancer [45, 46]. β-catenin is a key target in the Wnt/β-catenin signaling pathway that regulates tumor metastasis [47]. MMP1 is involved in multiple biological functions, and promotes cancer progression and poor outcome by regulating the invasion, metastasis and angiogenesis [48]. Knockdown of FOSL1 significantly inhibited the expression of CDH2, β-catenin, VIM and MMP1, and promoted the expression of CDH1. The effect of FOSL1 on the expression of these genes proves that FOSL1 promotes the invasion and metastasis of pancreatic cancer. Overexpression of

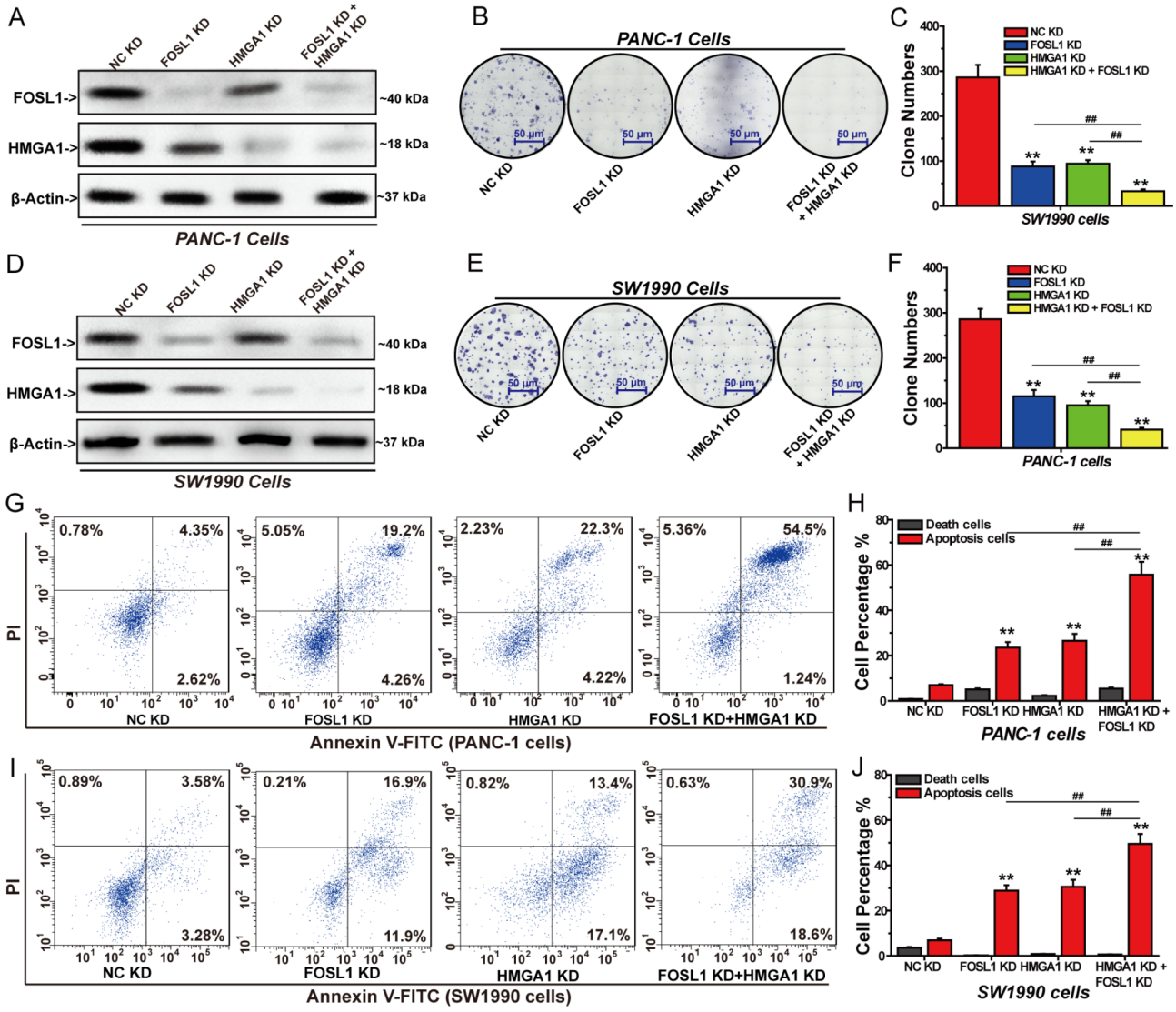

Fig. 9 FOSL1 and HMGA1 combined effects on the proliferation of pancreatic cancer cells. (**A**) The expression of FOSL1 and HMGA1 in PANC-1 cells analyzed by Western blots. (**B**) Effects of FOSL1 and HMGA1 on the formation of PANC-1 clones. (**C**) Numbers of PANC-1 clones in each group. (**D**) The expression of FOSL1 and HMGA1 in SW1990 cells analyzed by Western blots. (**E**) Effects of FOSL1 and HMGA1 on the formation of SW1990 clones. (**F**) Numbers of SW1990 clones in each group. (**G**) Effects of FOSL1 and HMGA1 on the apoptosis of PANC-1 cells. (**H**) Percentage of apoptosis of PANC-1 cells. (**I**) Effects of FOSL1 and HMGA1 on the apoptosis of SW1990 cells. (**J**) Percentage of apoptosis of SW1990 cells. The results from three independent experiments were statistically analyzed using one way ANOVA: $^{*}P<0.05$, $^{**}P<0.01$ compared with control group, $^{*}P<0.05$, $^{**}P<0.01$ compared with control group, $^{\#}P<0.05$, $^{\#\#}P<0.01$ compared with FOSL1 KD combined with HMGA1 KD group

multidrug efflux systems is an important cause of drug resistance in cancer cells, which is closely associated with the poor prognosis of cancer [49]. Membrane ABC transporters, including ABCB1, ABCC1, ABCC4, ABCG1 and ABCG2, eject anticancer drugs to reduce the sensitivity of cancer cells to drugs [49–51]. Silencing FOSL1 expression significantly inhibited the expression of these membrane ABC transporters to promote multidrug resistance in cancer cells. A series of regulatory effects of FOSL1 on stemness, invasion and metastasis, and multidrug efflux system suggest that FOSL1 is a key driving target for the malignant progression and poor prognosis of pancreatic cancer. Targeting FOSL1 has the potential to improve survival and quality of life for patients with pancreatic cancer.

Among these important targets regulated by FOSL1, we found that HMGA1 expression was positively correlated to FOSL1 expression. Meanwhile, HMGA1 was overexpressed in pancreatic cancer, which was negatively correlated with patient survival and positively correlated with poor prognosis. Further RNA sequencing and co-IP Mass spectrometry analysis showed that HMGA1 was a crucial target that regulated by FOSL1 and directly interacted with FOSL1. Q-PCR of ChIP confirmed that the

promoter of HMGA1 directly binds to FOSL1. HMGA1 is directly regulated by FOSL1 at the transcriptional level. Further experiments confirmed that FOSL1 promoted the proliferation of pancreatic cancer cells by promoting HMGA1 expression. HMGA1 is a nonhistone chromatin structural protein that is overexpressed in various cancers and is associated with cancer occurrence, malignant progression and poor prognosis [21–23]. HMGA1 is an oncogene that promotes stemness, invasion and metastasis, drug resistance, immunosuppression, and cell cycle progression through multiple signaling pathways [24–30]. Indeed, HMGA1 regulated the expression of genes involved in cell stemness, EMT, and multidrug efflux systems. Knockdown of HMGA1 inhibited the proliferation, stemness, invasion and migration, and drug resistance of pancreatic cancer cells, and promoted the apoptosis of pancreatic cancer cells. Moreover, targeted inhibition of FOSL1 and HMGA1 expression significantly inhibited the proliferation of pancreatic cancer cells. Targeting FOSL1 and HMGA1 simultaneously may lead to an effective treatment for pancreatic cancer.

Conclusions

In summary, we clarified the mechanism for the effect of FOSL1 on the proliferation of challenging pancreatic cancer in vitro and in vivo. FOSL1 is overexpressed in pancreatic cancer cells and closely correlated with the poor survival and prognosis of patients with pancreatic cancer. FOSL1 promotes the malignant proliferation and progression of pancreatic cancer by regulating stemness, invasion and metastasis, and multidrug efflux system. HMGA1 is a crucial downstream target regulated by FOSL1 at the transcriptional level and directly interacts with FOSL1 to promote the malignant progression of pancreatic cancer. HMGA1 regulates the expression of genes related to cell stemness, EMT, and multidrug efflux systems to promote the proliferation of pancreatic cancer cells. Targeted inhibition of FOSL1 and HMGA1 expression significantly inhibited the proliferation of pancreatic cancer cells. Targeting FOSL1 and HMGA1 in monotherapy or combination therapy is a promising strategy for the treatment of advanced and metastasis pancreatic cancer.

Supplementary Information

The online version contains supplementary material available at https://doi.org/10.1186/s12967-025-06304-w .

Supplementary Material 1

Supplementary Material 2

Acknowledgements

This work was supported by Lanzhou University New medical innovation platform and Key Lab of Preclinical Study for New Drugs of Gansu Province (Lanzhou, Gansu, China). We are grateful for the sequencing platform and bioinformation analysis of Gene Denovo Biotechnology Co., Ltd (Guangzhou, Guangdong, China), the support of animal experiments of OG pharmaceutical Technology Co., Ltd (Nanjing, Jiangsu, China).

Author contributions

SPW and YLL conceived, designed, and supervised this study. XLL, XYZ, TYZ performed the phenotypic experiments in vitro and in vivo. SPW, XLL and XYZ analyzed bioinformation data and RNA sequencing data. XLL, XYZ TYZ, YLC and LY performed molecular biological experiments. XLL and XYZ analyzed and prepared the figures. SPW, YLL, XLL and XYZ prepared the manuscription.

Funding

This research was supported by the National Natural Science Foundation of China (Grant No. 82104206, No. 82373890 and No. 82460017), and the open project of the Key Laboratory of Preclinical Study for New Drugs of Gansu Province.

Data availability

The data presented in this study is available on reasonable request from the corresponding author.

Declarations

Ethics approval

According to the Declaration of Helsinki, the Ethics Committee of Lanzhou University (D2022-224) has approved this study.

Informed consent

Written informed consent was not applicable.

Conflict of interest

The authors declare no competing interests.

Author details

[1]The First School of Clinical Medicine, Lanzhou University, Lanzhou 730000, PR China
[2]Key Laboratory of Preclinical Study for New Drugs of Gansu Province, Institute of Biochemistry and Molecular Biology, School of Basic Medical Sciences, Lanzhou University, Lanzhou 730000, PR China
[3]Medical College of Guizhou University, Guiyang 550025, Guizhou Province, China

Received: 24 September 2024 / Accepted: 23 February 2025
Published online: 04 March 2025

References

1. Zhao Z, Liu W. Pancreatic cancer: A review of risk factors, diagnosis, and treatment. Technol Cancer Res Treat. 2020;19.
2. Stoffel EM, Brand RE, Goggins M. Pancreatic cancer: changing epidemiology and new approaches to risk assessment, early detection, and prevention. Gastroenterology. 2023;164:752–65.
3. Kolbeinsson HM, Chandana S, Wright GP, Chung M. Pancreatic cancer: A review of current treatment and novel therapies. J Invest Surg. 2023;36:2129884.
4. Rehman M, Khaled A, Noel M. Cytotoxic chemotherapy in advanced pancreatic Cancer. Hematol Oncol Clin North Am. 2022;36:1011–8.
5. Stoop TF, Theijse RT, Seelen LWF, Groot Koerkamp B, van Eijck CHJ, Wolfgang CL, et al. Preoperative chemotherapy, radiotherapy and surgical decision-making in patients with borderline resectable and locally advanced pancreatic cancer. Nat Rev Gastroenterol Hepatol. 2024;21:101–24.
6. Xing L, Lv L, Ren J, Yu H, Zhao X, Kong X, et al. Advances in targeted therapy for pancreatic cancer. Biomed Pharmacother. 2023;168:115717.
7. Zhu H, Wei M, Xu J, Hua J, Liang C, Meng Q, et al. PARP inhibitors in pancreatic cancer: molecular mechanisms and clinical applications. Mol Cancer. 2020;19:49.
8. Luo J. KRAS mutation in pancreatic cancer. Semin Oncol. 2021;48:10–8.
9. Sotorasib Tackles. KRASG12C-Mutated pancreatic Cancer. Cancer Discov. 2022;12:878–9.

10. Song D, Lian Y, Zhang L. The potential of activator protein 1 (AP-1) in cancer targeted therapy. Front Immunol. 2023;14:1224892.
11. Jiang X, Xie H, Dou Y, Yuan J, Zeng D, Xiao S. Expression and function of FRA1 protein in tumors. Mol Biol Rep. 2020;47:737–52.
12. Sobolev VV, Khashukoeva AZ, Evina OE, Geppe NA, Chebysheva SN, Korsunskaya IM, et al. Role of the transcription factor FOSL1 in organ development and tumorigenesis. Int J Mol Sci. 2022;23:1521.
13. Khedri A, Guo S, Ramar V, Hudson B, Liu M. FOSL1's oncogene roles in glioma/glioma stem cells and tumorigenesis: A comprehensive review. Int J Mol Sci. 2024;25:5362.
14. Casalino L, Talotta F, Matino I, Verde P. FRA-1 as a regulator of EMT and metastasis in breast Cancer. Int J Mol Sci. 2023;24:8307.
15. Guo S, Ramar V, Guo AA, Saafir T, Akpobiyeri H, Hudson B, et al. TRPM7 transactivates the FOSL1 gene through STAT3 and enhances glioma stemness. Cell Mol Life Sci. 2023;80:270.
16. Liu G, Wang H, Ran R, Wang Y, Li Y. FOSL1 transcriptionally regulates PHLDA2 to promote 5-FU resistance in colon cancer cells. Pathol Res Pract. 2023;246:154496.
17. Li L, Wang N, Xiong Y, Guo G, Zhu M, Gu Y. Transcription factor FOSL1 enhances drug resistance of breast Cancer through DUSP7-Mediated dephosphorylation of PEA15. Mol Cancer Res. 2022;20:515–26.
18. Vallejo A, Perurena N, Guruceaga E, Mazur PK, Martinez-Canarias S, Zandueta C et al. An integrative approach unveils FOSL1 as an oncogene vulnerability in KRAS-driven lung and pancreatic cancer. Nat Commun. 2017;8:14294.
19. Li AL, Sugiura K, Nishiwaki N, Suzuki K, Sadeghian D, Zhao J, et al. FRA1 controls acinar cell plasticity during murine KrasG12D-induced pancreatic acinar to ductal metaplasia. Dev Cell. 2024;59:3025–e30427.
20. Dai C, Rennhack JP, Arnoff TE, Thaker M, Younger ST, Doench JG et al. SMAD4 represses FOSL1 expression and pancreatic cancer metastatic colonization. Cell Rep. 2021;36:109443.
21. Wang L, Zhang J, Xia M, Liu C, Zu X, Zhong J. High mobility group A1 (HMGA1): structure, biological function, and therapeutic potential. Int J Biol Sci. 2022;18:4414–31.
22. Wang T, Zhou T, Fu F, Han Y, Li Y, Yuan M. HMGA1 as a potential prognostic and therapeutic biomarker in breast Cancer. Dis Markers. 2022;2022:7466555.
23. Pádua D, Pinto DF, Figueira P, Pereira CF, Almeida R, Mesquita P. HMGA1 has predictive value in response to chemotherapy in gastric Cancer. Curr Oncol. 2021;29:56–67.
24. Yang Q, Wang Y, Li M, Wang Z, Zhang J, Dai W, et al. HMGA1 promotes gastric cancer growth and metastasis by transactivating SUZ12 and CCDC43 expression. Aging. 2021;13:16043–61.
25. Chang X, Liu J, Yang Q, Gao Y, Ding X, Zhao J, et al. Targeting HMGA1 contributes to immunotherapy in aggressive breast cancer while suppressing EMT. Biochem Pharmacol. 2023;212:115582.
26. Zheng Q, Luo Z, Xu M, Ye S, Lei Y, Xi Y. HMGA1 and FOXM1 cooperate to promote G2/M cell cycle progression in Cancer cells. Life (Basel Switzerland). 2023;13:1225.
27. Chen M, Xu K, Li B, Wang N, Zhang Q, Chen L, et al. HMGA1 regulates the stem Cell-Like properties of Circulating tumor cells from GIST patients via Wnt/β-Catenin pathway. Onco Targets Ther. 2020;13:4943–56.
28. Cheng Y, Cheng T, Zhao Y, Qu Y. HMGA1 exacerbates tumor progression by activating miR-222 through PI3K/Akt/MMP-9 signaling pathway in uveal melanoma. Cell Signal. 2019;63:109386.
29. Liu X, Zhou Z, Wang Y, Zhu K, Deng W, Li Y, et al. Downregulation of HMGA1 mediates autophagy and inhibits migration and invasion in bladder Cancer via miRNA-221/TP53INP1/p-ERK Axis. Front Oncol. 2020;10:589.
30. Chia L, Wang B, Kim J-H, Luo LZ, Shuai S, Herrera I, et al. HMGA1 induces FGF19 to drive pancreatic carcinogenesis and stroma formation. J Clin Invest. 2023;133:151601.
31. Guo S, Zhao W, Zhang T, Li S, Guo J, Liu L. Identification of a ferroptosis-related gene signature for prognosis prediction in colorectal cancer patients and relationship with vitamin D. J Steroid Biochem Mol Biol. 2023;227:106234.
32. Wang S-P, Wu S-Q, Huang S-H, Tang Y-X, Meng L-Q, Liu F, et al. FDI-6 inhibits the expression and function of FOXM1 to sensitize BRCA-proficient triple-negative breast cancer cells to Olaparib by regulating cell cycle progression and DNA damage repair. Cell Death Dis. 2021;12:1138.
33. Wu S-Q, Huang S-H, Lin Q-W, Tang Y-X, Huang L, Xu Y-G, et al. FDI-6 and Olaparib synergistically inhibit the growth of pancreatic cancer by repressing BUB1, BRCA1 and CDC25A signaling pathways. Pharmacol Res. 2022;175:106040.
34. Tuccitto A, Beretta V, Rini F, Castelli C, Perego M. Melanoma stem cell sphere formation assay. Bio-protocol. 2017;7:e2233.
35. Wang J, Zhang J, Liu H, Meng L, Gao X, Zhao Y et al. N6-methyladenosine reader hnRNPA2B1 recognizes and stabilizes NEAT1 to confer chemoresistance in gastric cancer. Cancer Commun (London, England). 2024;44:469–90.
36. Wei Y, Li Y, Chen Y, Liu P, Huang S, Zhang Y, et al. ALDH1: A potential therapeutic target for cancer stem cells in solid tumors. Front Oncol. 2022;12:1026278.
37. Zhu M, Fan H, Deng J, Jiang K, Liao J, Zhang X, et al. BMI1 Silencing liposomes suppress postradiotherapy Cancer stemness against radioresistant hepatocellular carcinoma. ACS Nano. 2023;17:23405–21.
38. Parisi S, Piscitelli S, Passaro F, Russo T. HMGA proteins in stemness and differentiation of embryonic and adult stem cells. Int J Mol Sci. 2020;21:362.
39. Nimmakayala RK, Seshacharyulu P, Lakshmanan I, Rachagani S, Chugh S, Karmakar S, Rauth S, Vengoji R, Atri P, Talmon GA, Lele SM, Smith LM, Thapa I, Bastola D, Ouellette MM, Batra SK, Ponnusamy MP. Cigarette Smoke Induces Stem Cell Features of Pancreatic Cancer Cells via PAF1. Gastroenterology. 2018 Sep;155(3):892-908.e6.Nimmakayala RK, Seshacharyulu P, Lakshmanan I, Rachagani S, Chugh S, Karmakar S et al. JG Wakefield CA Moores editors. 2018 Cigarette smoke induces stem cell features of pancreatic Cancer cells via PAF1. Gastroenterology 155 892–908 e6.
40. Lau EYT, Lo J, Cheng BYL, Ma MKF, Lee JMF, Ng JKY et al. Cancer-associated fibroblasts regulate tumor-initiating cell plasticity in hepatocellular carcinoma through c-Met/FRA1/HEY1 signaling. Cell Rep. 2016;15:1175–89.
41. Wang Y, Hu Q, Cao Y, Yao L, Liu H, Wen Y et al. FOSL1 promotes stem cell–like characteristics and anoikis resistance to facilitate tumorigenesis and metastasis in osteosarcoma by targeting SOX2. Int J Mol Med. 2024;54:94.
42. Wang T, Song P, Zhong T, Wang X, Xiang X, Liu Q et al. The inflammatory cytokine IL-6 induces FRA1 deacetylation promoting colorectal cancer stem-like properties. Oncogene. 2019;38:4932–47.
43. Zhou J, Chen S, Liu J, Du J, Li J. Knockdown of HnRNPAB reduces the stem cell properties and enhances the chemosensitivity of human colorectal cancer stem cells. Oncol Rep. 2023;49:23405–21.
44. Hu Y, Li Z, Gong L, Song Z. β-Asarone suppresses TGF-β/Smad signaling to reduce the invasive properties in esophageal squamous cancer cells. Med Oncol. 2022;39:243.
45. Paolillo M, Schinelli S. Extracellular matrix alterations in metastatic processes. Int J Mol Sci. 2019;20:4947.
46. Xiong Y, Zu X, Wang L, Li Y, Chen M, He W, et al. The VIM-AS1/miR-655/ZEB1 axis modulates bladder cancer cell metastasis by regulating epithelial-mesenchymal transition. Cancer Cell Int. 2021;21:233.
47. Zhang Y, Wang X. Targeting the Wnt/β-catenin signaling pathway in cancer. J Hematol Oncol. 2020;13:165.
48. Kurnia I, Rauf S, Hatta M, Arifuddin S, Hidayat YM, Natzir R, et al. Molecular Patho-mechanisms of cervical cancer (MMP1). Ann Med Surg. 2022;77:103415.
49. Yalcin-Ozkat G. Molecular modeling strategies of Cancer multidrug resistance. Drug Resist Updat. 2021;59:100789.
50. Dean M, Moitra K, Allikmets R. The human ATP-binding cassette (ABC) transporter superfamily. Hum Mutat. 2022;43:1162–82.
51. Zeng G-G, Lei Q, Jiang W-L, Zhang X-X, Nie L, Gong X, et al. A new perspective on the current and future development potential of ABCG1. Curr Probl Cardiol. 2024;49:102161.

Publisher's note